

NCSX

Field Error Source Assessment Notebook

Rev 0

19 September 2003

Prepared by:

A. Brooks

Table of Contents

1	INTRODUCTION.....	1
1.1	PURPOSE	1
1.2	SCOPE.....	1
1.3	APPLICABLE DOCUMENTS	1
1.3.1	NCSX Documents	1
2	DESCRIPTION OF METHODS.....	1
3	FIELD ERROR SOURCES.....	6
3.1	COILS (MODULAR/PF/TF).....	6
3.1.1	Fabrication and Assembly Tolerances	6
3.1.2	Leads and Turn Transitions	36
3.1.3	Modular Leads	38
3.2	EDDY CURRENTS.....	41
3.2.1	Modular Coil Support Structure	41
3.2.2	Vacuum Vessel	48
3.2.3	Existing Copper Floor (Ground Plane).....	50
3.2.4	Machine Base Plates	51
3.3	FERROMAGNETIC MATERIAL.....	51
3.3.1	Neutral Beam Magnets	51
3.3.2	Building Steel (TBD).....	56
3.3.3	Other (TBD)	56
3.4	DIAGNOSTICS (TBD)	56

Table of Figures

Figure 1	Evaluation of Island Size in the VACISLD Code using VMEC Field	3
Figure 2	VMEC Resonant Surfaces in LI383 Fixed Boundary Plasma	3
Figure 3	Benchmark of VACISLD and TraceBrtp Codes with PIES.....	4
Figure 4	Benchmark of VACISLD and TraceBrtp Codes with PIES.....	5

1 INTRODUCTION

1.1 PURPOSE

This document has been prepared for the National Compact Stellarator Experiment (NCSX) Project to identify and track potential sources of field errors and assess their impact on magnetic field quality at the plasma.

1.2 SCOPE

This document includes but is not limited to sources of field errors from all magnetic field coils, from eddy currents in both machine components and buildings structures induced during machine operation, and from the presence of ferromagnetic material both permanently magnetized and induced/inductively magnetized by other field sources. It does not attempt to include field errors arising from the plasma itself.

The assessment of impact on magnetic field quality implies evaluating the magnetic field perturbation for each source at the plasma, and estimating the volume of plasma lost to magnetic islands using a linear perturbation vacuum field predictor. The island size estimate is strictly valid only for vacuum fields and is intended to provide a first cut assessment. A more rigorous analytical assessment of island size for current carrying plasmas requires use of the PIES code, which is beyond the scope of this document.

For field errors from eddy currents, an assessment is assumed needed only if the time constants for current decay fail to meet, or are not covered by, the General Requirements Document (GRD). The GRD imposes a 10 ms requirement for Vacuum Vessel and In-Vessel structures or 20 ms for structures outside the Vacuum Vessel and inside the Cryostat.

1.3 APPLICABLE DOCUMENTS

1.3.1 NCSX Documents

General Requirements Document (NCSX-ASPEC-GRD-01)

2 DESCRIPTION OF METHODS

The impact of field errors are traditionally investigated for vacuum field configurations by examining Poincare plots from field line tracing for any source and observing induced islands or changes in islands with respect to a Poincare plot for an ideal configuration. For NCSX, operating with significant plasma current and beta, the field from the plasma must be included to achieve the iota profiles expected which cross the resonances of concern. The PIES code can be used to produce Poincare plots which are self-consistent and indeed is being used for necessarily limited investigations within the NCSX Physics Group. The long run times required for convergence and limitations regarding symmetry-breaking perturbations make PIES a difficult design tool to employ for general engineering use.

A simpler approach was taken to provide a first cut at field error source assessment. It is based on the analytic expression for magnetic island width, in flux coordinates, by magnetic field perturbations in a general toroidal stellarator geometry¹. It presumes the underlying (perturbation free) field contains nested magnetic surfaces and is valid for rational surfaces (where the rotational transform $\iota = n/m$). The VMEC equilibrium provides such a field. (Alternately, a

vacuum configuration with the same rotational transform profile as the LI383 full current, full beta configuration could be used. However, attempts to define such a configuration were not successful.) Use of the VMEC equilibrium simplifies the evaluation of the island width which depends on B^s/B^ϕ expressed in straight line (magnetic) coordinates. Figure 1 presents the method used.

A computer program called VACISLD was written to evaluate the island width using the VMEC field and a perturbation field generated by coil filaments or alternately supplied as a field map from other sources. A field line tracing routine called TraceBrtp, capable of tracing the perturbation field with the VMEC field in VMEC coordinates, was developed to examine both symmetric and symmetry breaking field perturbations. VACISLD and TraceBrtp were benchmarked against PIES* for symmetry preserving field perturbations (*PIES was modified by Don Monticello to allow adding a perturbation field from coils to the background VMEC field). Figure 2 shows the resonances targeted.

The Field Error Source Assessment Methodology is similar for each of the sources identified. For each field error source, a field map is generated on resonant surfaces in the reference plasma using methods appropriate for the source. For coils which provide the sustaining field to form and support the plasma, the field error map is the difference between the ideal coil configuration and the perturbed or actual coil configuration, and the field is calculated using direct Biot-Savart integration of line filaments. For eddy currents, the total field is used and it is calculated by the SPARK code as field at remote points. For ferromagnetic sources, the ANSYS code is used to both determine the magnetization of the ferromagnetic source from other participating field sources and calculate the field at the plasma from the magnetized ferromagnetic material.

Initial studies used the VMEC LI383 fixed boundary plasma configuration as the reference plasma. Subsequent work has used the latest VMEC free boundary plasma configurations (m45, m50, ...).

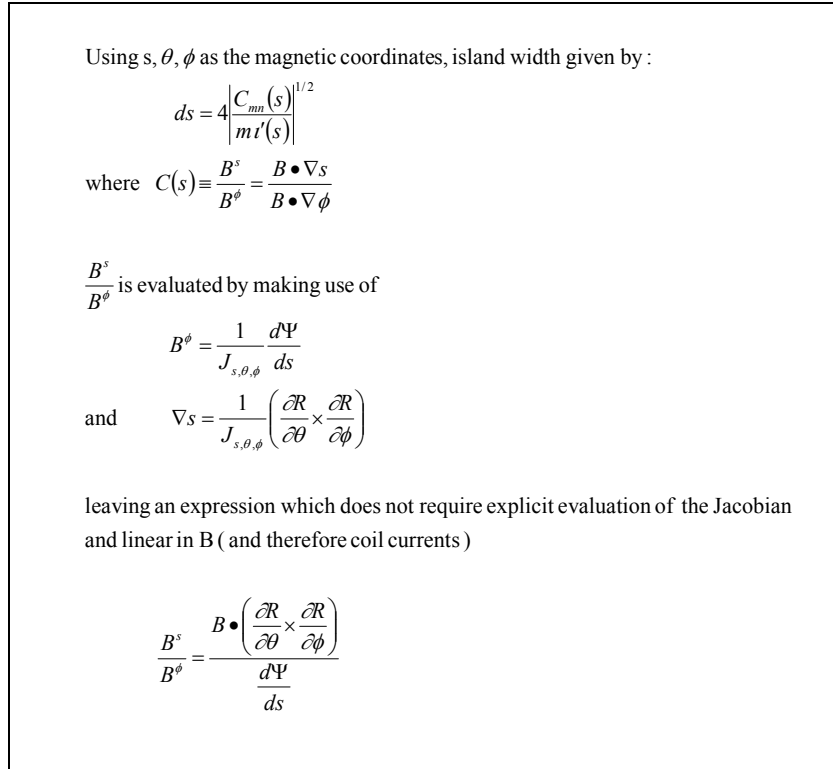


Figure 1 Evaluation of Island Size in the VACISLD Code using VMEC Field

Li383 Targeted Resonances

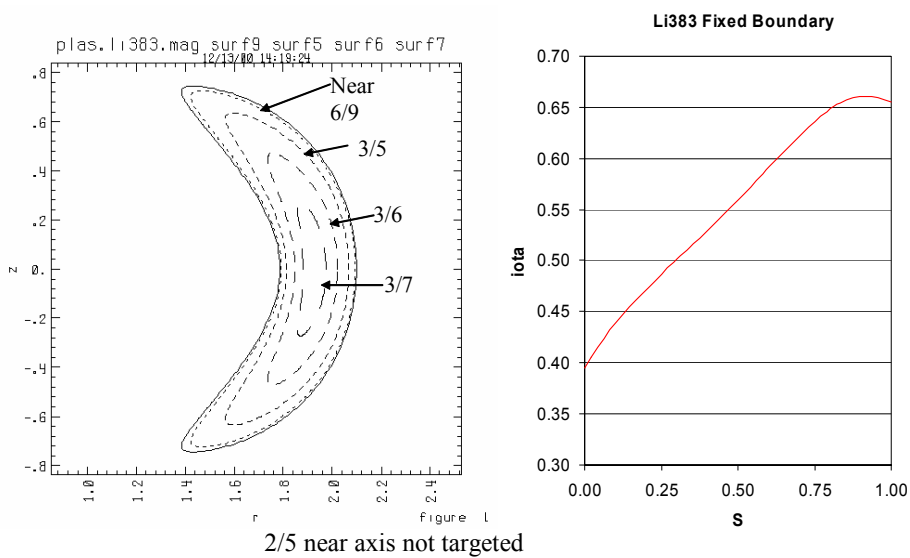
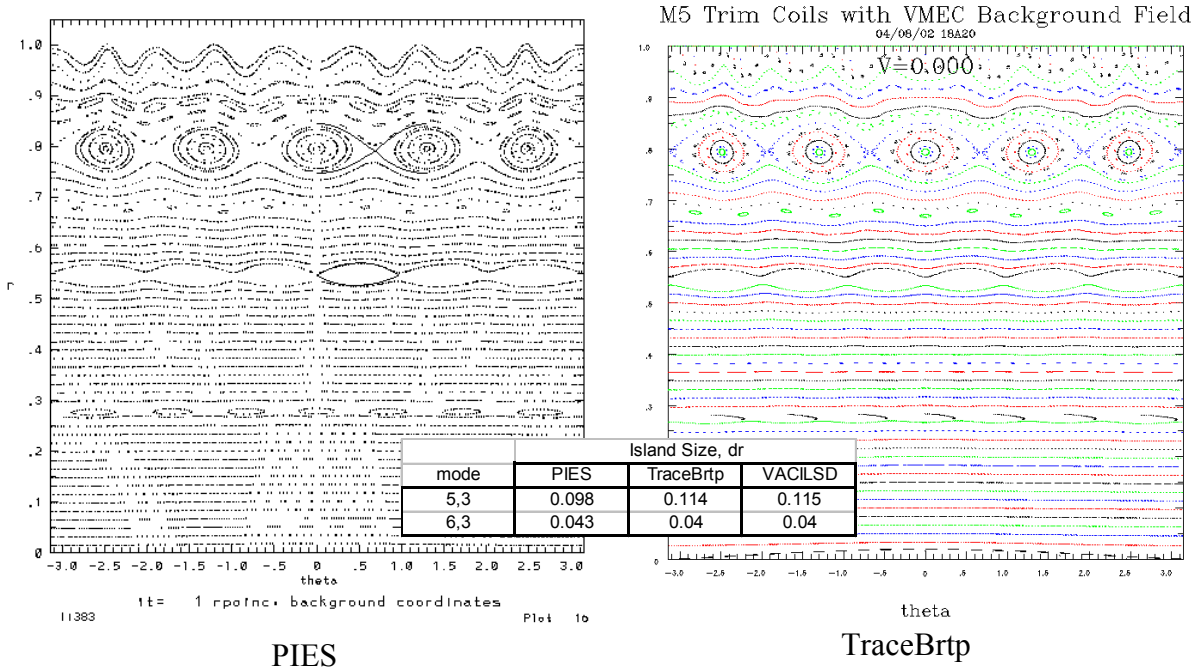


Figure 2 VMEC Resonant Surfaces in LI383 Fixed Boundary Plasma

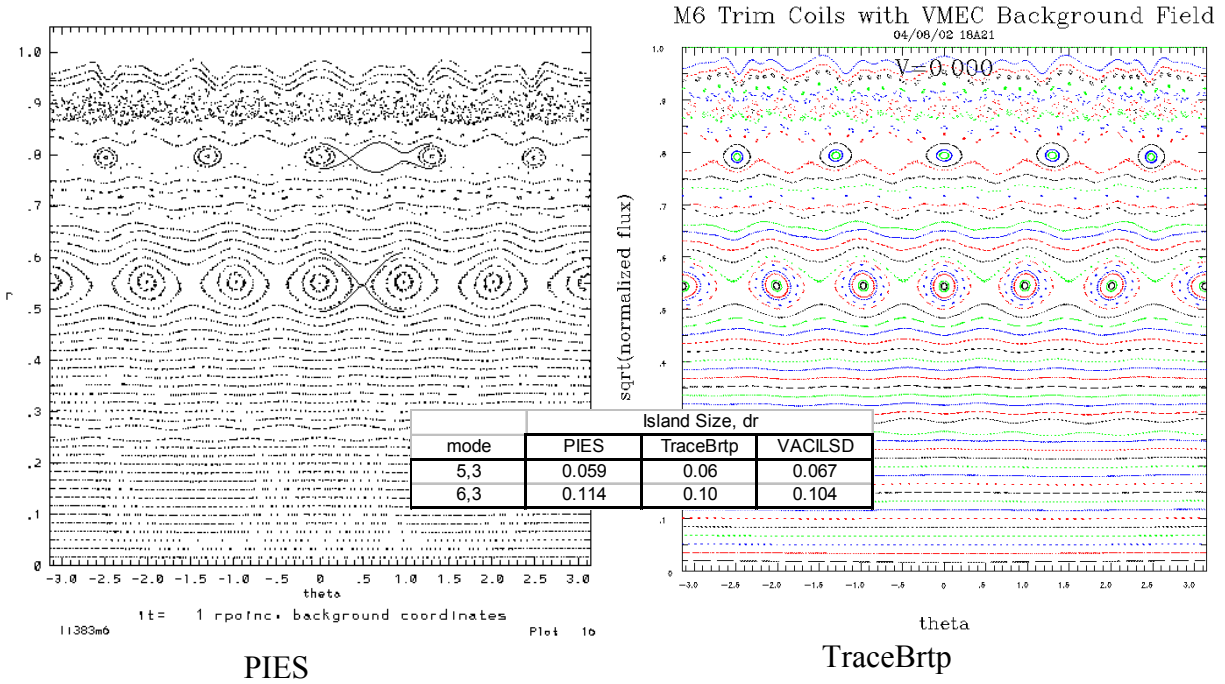
Benchmark of Field Line Tracing of Perturbation Field* from Coils on VMEC Field



*From 1 KA M5 Trim Coils

Figure 3 Benchmark of VACILSD and TraceBrtp Codes with PIES

Benchmark of Field Line Tracing of Perturbation Field* from Coils on VMEC Field



*From 1 KA M6 Trim Coils

Figure 4 Benchmark of VACISLD and TraceBrtp Codes with PIES

3 FIELD ERROR SOURCES

3.1 COILS (MODULAR/PF/TF)

3.1.1 Fabrication and Assembly Tolerances

The accuracy to which we can fabricate and assemble the field coils represents probably the biggest concern for field errors. It also posed a large challenge in how to assess and evaluate these inherent uncertainties beforehand.

The experience gained from the stellarator community in the construction of past machines suggested tolerances on the order of one in a thousand as installed were acceptable, though not necessarily cheaply. Applying this to NCSX with a major radius of ~ 1.5 m would say tolerances of ± 1.5 mm would be required. Subsequent discussions with potential manufacturers and construction groups have given us confidence that this is achievable. The question remained whether this is adequate from a field error viewpoint.

To explore the impact of coil tolerances or more generally, the impact of geometric changes to the coil windings, a large number of potential coil distortions were examined using the methods described in Section 1.3.

First, to try and reflect fabrication tolerances, systematic perturbations were applied to each degree of freedom describing the coil geometry. This was done for both the individual coil types (i.e. modular coil types A, B and C; TF 1, 2 and 3; and PF 1 through PF 6) and the coil systems collectively. The perturbations were sinusoidal variations (where the mode number and phase of the variation were also varied) in r , θ and z . A coil set containing the perturbed geometry has combined with a coil set of opposite current of the unperturbed geometry, resulting in a coil set which provided only the differential field (i.e. error field) which could be evaluated against the VMEC fixed or free boundary equilibrium background field. For each geometric perturbation applied, an evaluation of the magnetic island size induced at each (significant) resonant surface in the plasma was made. Results of this are contained in the figures which follow, taken from earlier presentations. Results are for each perturbation taken alone, where the magnitude of the perturbation is the full tolerance. A large number of cases were examined to cover the different coils and groups of coils, degree of freedom, mode and phase of perturbation.

Second, to try and reflect assembly tolerances, again systematic perturbations were applied to each degree of freedom describing the coil position and orientation (i.e. free body displacements). Again the effect on individual coil types and coil systems collectively were explored. The degree of freedom changes were done relative to a local coordinate system at the center of gravity of the coil. Rotation magnitudes were chosen to limit the maximum displacement at the coil to the specified tolerance. (Note: Some of the initial work contained herein reflected an earlier 2.0 mm tolerance instead the present 1.5 mm)

Examination of the impact of these various individual perturbations showed significant variation in impact on island size.

To try to assess how these different perturbations from fabrication and assembly might combine, a method was devised to combine them in a random fashion. A random factor was applied to coordinate change resulting from each combination of different coils and groups of coils, degree of freedom, mode and phase of perturbation. The individual coordinate changes were then

summed and the resultant coordinate changes (now effectively a random function) normalized to the 1.5 mm tolerance specified. (This assumes the stack up of tolerances from all sources will be such as to assure the final location of every point in every coil is within +/- 1.5 mm) A large number of random functions were examined and the distribution of island sizes observed. Results are plotted and tabulated in the figures that follow.

What should be clear is that even at these tight tolerances, the islands produced from either systematic or random distributions of coil geometry errors are potentially damaging, possibly exceeding 20% of total flux in plasma. This would be unacceptable without some form of mitigation.

A set of in-vessel trim coils was previously designed to handle symmetry-preserving corrections, targeting the 3/5 ($m=5$) and 3/6 ($m=6$) resonances. Another set of ex-vessel trim coils was introduced to target lower order, non-symmetric resonances (1/2, 2/4, 2/3, etc). These are pictured in the figures that follow.

To demonstrate their effectiveness in island mitigation, a number of the more severe cases of islands induced from coil geometric perturbations were examined. For each case, currents in each of the trim or correction coils need to be solved for to attempt to suppress the islands without undue damage to the plasma boundary or exciting other resonances. A coupling matrix (**A**) was calculated which related unit currents in each of the trim/correction coils to impact on the resonant field component for each resonance. A target vector (**b**) was formed of the resonances induced by the coil geometry perturbation that we are trying to suppress. The trim/correction coil current vector (**x**) is obtained by solving $\mathbf{Ax}=\mathbf{b}$ using a SVD (single value decomposition) algorithm. The TraceBrtp code described earlier was used to visualize the field structure before and after the applied correction. Results, shown in the figures that follow, indicate even for the worse case stack ups at 1.5 mm tolerance, the total flux lost to islands can be reduced to an acceptable level without undue perturbations to the plasma boundary with acceptable current levels in the trim coils.

Not content to leave well enough alone, we tried to answer the question can we soften the tolerances (and simplify – i.e. reduce cost of – fabricating the coils). This question was examined by re-doing the random function studies using varying the tolerance values for the each of the coil systems (Modular, TF and PF) and within the Modular Coils. It was shown that tolerance control on the modular coils is most critical for regions of the coils that are in close proximity to the plasma, but could possibly be relaxed in regions far from the plasma. It was also shown that the tolerance of the TF and PF could be relaxed without significantly impacting field errors. Again, keep in mind that in all cases, the field errors would be intolerable without the use of trim coils. The real question is how good are the trim coils, in terms of how large a field error they can correct without damaging or otherwise altering the plasma configuration.

Other issues addressed herein include investigations into other forms of geometric perturbations, in addition to sinusoidal and random Fourier functional distributions. This includes local perturbations (i.e. ‘wavelet’ type) and broad deformations (i.e. large regions of the coils perturbed in the same fashion).

Impact of Coil Tolerances on Magnetic Surface Quality

NCSX Conceptual Design Review

May 21-23, 2002

Art Brooks

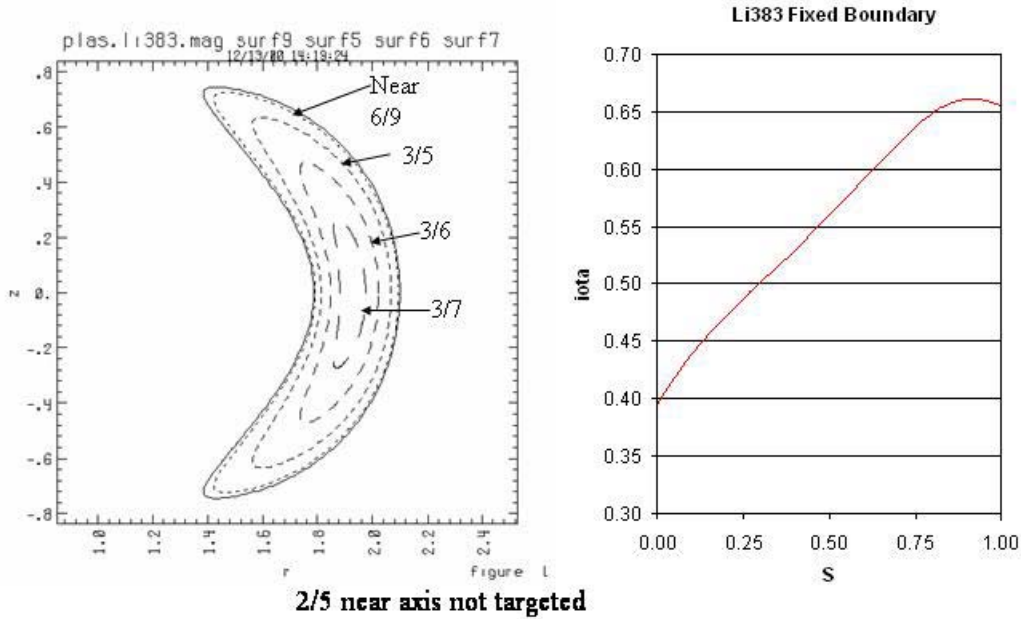
Overview

- The impact of coil tolerances on surface quality is studied by examining the effect of their field perturbations on magnetic surfaces in the plasma.
- A large number of coil fabrication and assembly errors investigated
 - Both systematic and random
 - Coil groups and individual coils
- A set of ex-vessel correction coils is introduced and their effectiveness in compensating for induced low order islands is demonstrated

Methods

- Field Perturbations are added to an island free plasma configuration (ie VMEC field + Δ coil field)
 - Note: Adding perturbation field to VMEC field for equilibria with plasma current and/or pressure is not self consistent
 - Perturbation Field = $B(\text{Deformed Coils}) - B(\text{Undeformed Coils})$
- An analytic predictor is used to predict island size (VACISLD)
- A field line tracing routine (TraceBrtp) capable of tracing the perturbation field with the VMEC field in VMEC coordinates was developed to examine both symmetric and symmetry breaking field perturbations
- VACISLD and TraceBrtp are benchmarked against PIES* for symmetry preserving field perturbations
 - *PIES was modified by Don Monticello to allow adding a perturbation field from coils to the background VMEC field

Li383 Targeted Resonances



Island Width Evaluation used in VACISLD using VMEC data

Using s, θ, ϕ as the magnetic coordinates, island width given by:

$$ds = 4 \left| \frac{C_{mn}(s)}{m i'(s)} \right|^{1/2}$$

where $C(s) \equiv \frac{B^s}{B^\phi} = \frac{B \cdot \nabla s}{B \cdot \nabla \phi}$

$\frac{B^s}{B^\phi}$ is evaluated by making use of

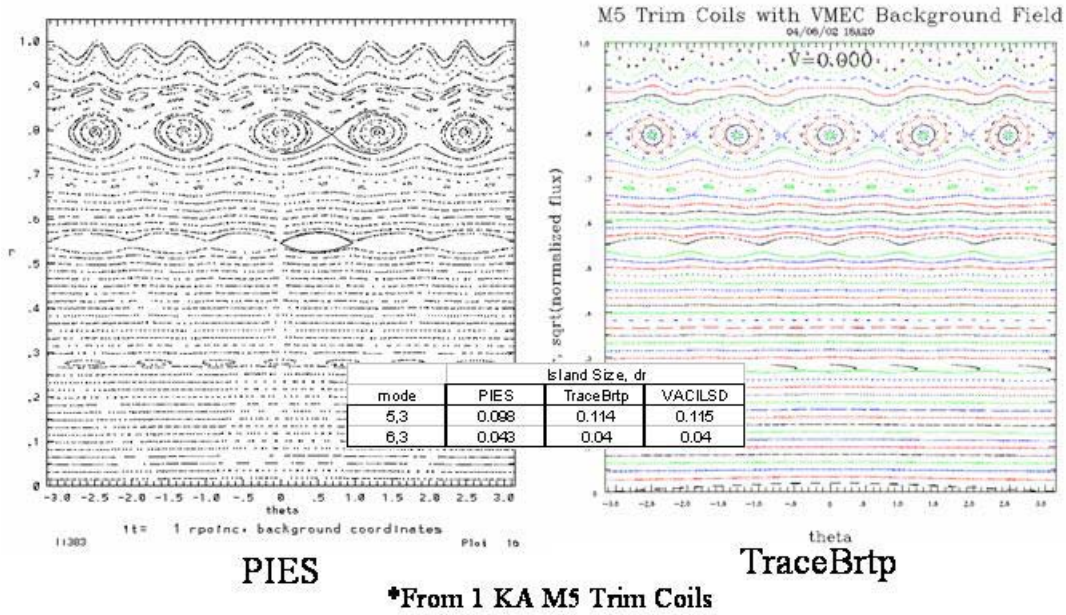
$$B^\phi = \frac{1}{J_{s,\theta,\phi}} \frac{dY}{ds}$$

and $\nabla s = \frac{1}{J_{s,\theta,\phi}} \left(\frac{\partial \mathcal{R}}{\partial \theta} \times \frac{\partial \mathcal{R}}{\partial \phi} \right)$

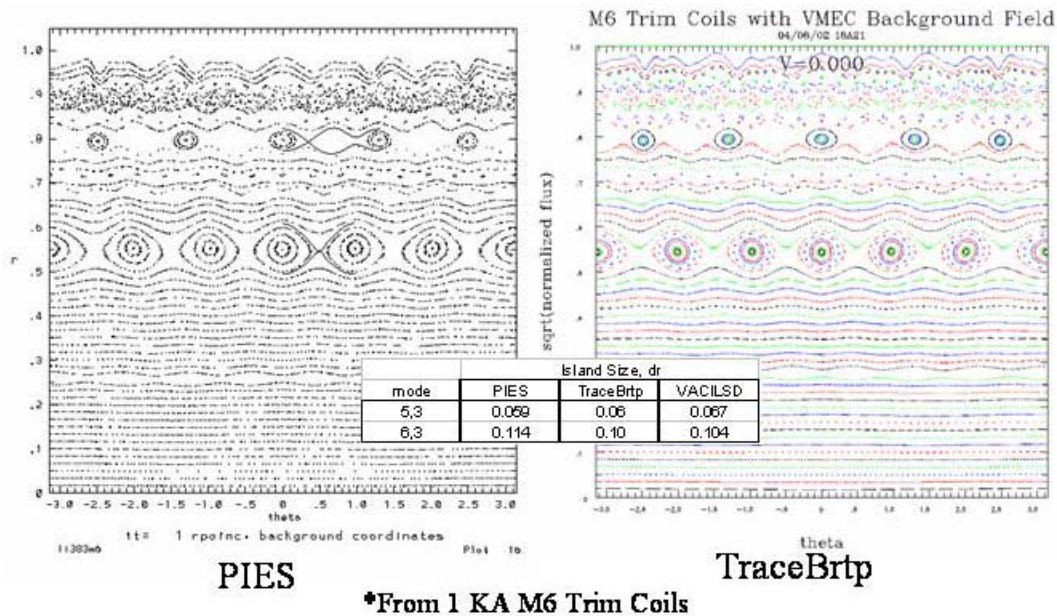
leaving an expression which does not require explicit evaluation of the Jacobian and linear in B (and therefore coil currents)

$$\frac{B^s}{B^\phi} = \frac{B \cdot \left(\frac{\partial \mathcal{R}}{\partial \theta} \times \frac{\partial \mathcal{R}}{\partial \phi} \right)}{\frac{dY}{ds}}$$

Benchmark of Field Line Tracing of Perturbation Field* from Coils on VMEC Field



Benchmark of Field Line Tracing of Perturbation Field* from Coils on VMEC Field



Definition of Systematic Errors

- **Coil distortion errors of the form**
 $\delta = \delta_m \sin(m \theta)$ and $\delta = \delta_m \cos(m \theta)$
applied to all Modular Coils collectively and individually
where δ represents r, θ , z coordinates of coil filaments
 - Similar distortions applied to TF Coils and Individual PFs

- **Coil assembly errors of the form**
 $\delta = \delta_m \sin(m \phi)$ and $\delta = \delta_m \cos(m \phi)$
applied to undistorted Modular Coil collectively
where δ represents r, θ , z coordinates of coil centroid plus coil rotations about each axis

- δ_m represents coil tolerance (2 mm for these studies, 1.5 mm for project)

Summary of Systematic Errors

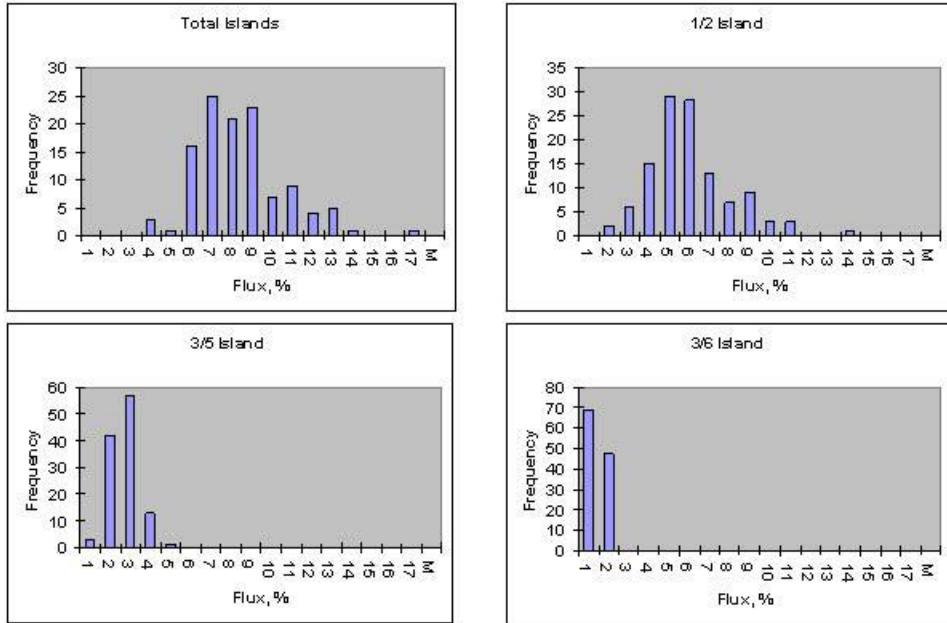
in Fabrication (coil distortion) and Assembly (free body displacement)

	Coil Distortion			Island		Coil Assembly			Island	
	Phase	Mode	DOF	Size	Resonance	Phase	Mode	DOF	Size	Resonance
All Modular	cos	3	dt	13.4%	3/5	cos	2	dz	18.7%	1/2
Modular 1	sin	2	dt	15.7%	1/2	-	-	dz	6.9%	1/2
Modular 2	cos	2	dt	12.6%	1/2	-	-	dz	9.9%	1/2
Modular 3	cos	2	dt	11.6%	1/2	-	-	rt	8.3%	1/2
All TF	cos	1	dt	1.0%	3/5	sin	1	rr	2.7%	1/2
TF 1	sin	2	dt	3.1%	1/2	-	-	rr	3.3%	1/2
TF 2	cos	2	dt	2.7%	1/2	-	-	rr	2.5%	1/2
TF 3	cos	2	dt	2.6%	1/2	-	-	dt	2.1%	1/2
PF1	sin	1	dz	3.7%	1/2	-	-	ry	3.7%	1/2
PF2	sin	1	dz	2.8%	1/2	-	-	ry	2.8%	1/2
PF3	sin	1	dz	2.8%	1/2	-	-	rx	2.8%	1/2
PF4	sin	1	dz	3.9%	1/2	-	-	rx	3.9%	1/2
PF5	sin	1	dr	2.9%	1/2	-	-	dy	2.9%	1/2
PF6	sin	1	dz	2.3%	1/2	-	-	ry	2.3%	1/2

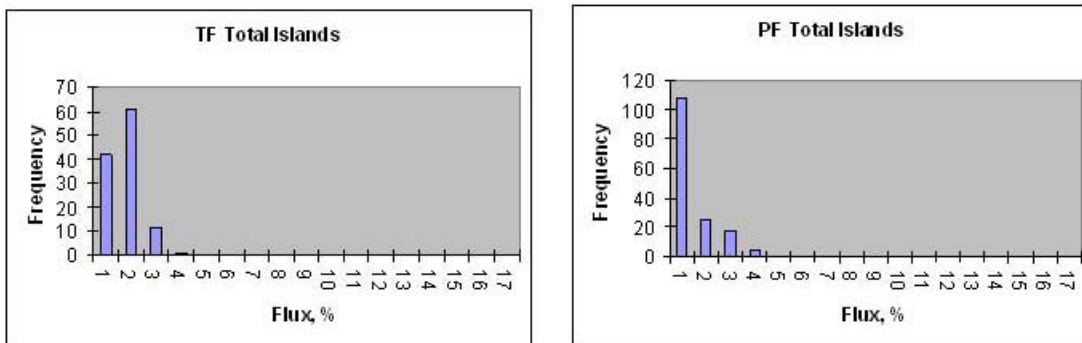
m=2 mode most significant, followed by m=5

Results for individual perturbations, not combined, with 2 mm tolerance

Frequency of Islands for Systematic Distortion of Individual Modular Coils



Frequency of Islands for Systematic Distortion of Individual TF & PF Coils



Symmetric Systematic Errors

- The worst case systematic error of an individual Modular Coil (15.7% 1/2 island at $\delta = 2$ mm) used to study effect of symmetric systematic errors in Modular Coil Group
 - all 6 symmetric images given same deformation
- Results show no 1/2 island (since errors are stellarator symmetric) but larger $m=5$ and $m=6$ islands. Total Flux in Islands less than individual case (13.4% vs 16.5% at $\delta = 1.5$ mm)
- More on this later...

Approach for Combining Tolerances (ie Applying Random Errors)

- Random Perturbation of Fourier Coefficients describing Coil Distortions (three coordinates)
$$\delta = \sum \delta_{m,s} \sin(m \theta) + \delta_{m,c} \cos(m \theta)$$
- Random Perturbation of six degrees of freedom describing coil assembly
- Final Displacements of each point in coil normalized to $\delta = 1.5$ mm max for each coil (Modular, TF and PF)

Island Sizes from Random Combinations Only Slightly Larger than Systematic Errors of Individual or Collective Coils

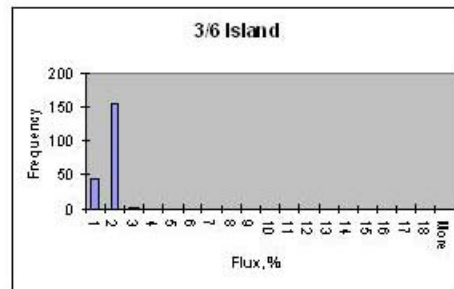
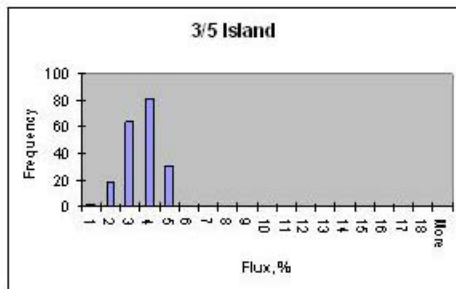
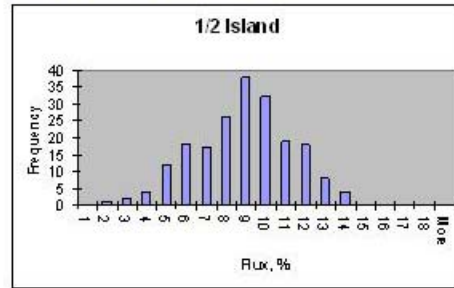
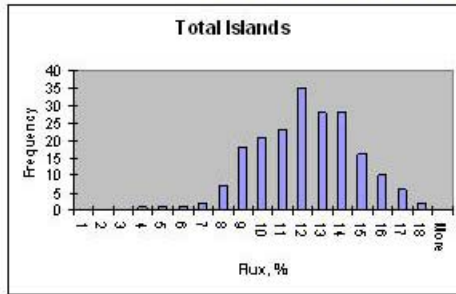
Distribution of Island Sizes vs Mode Numbers									
Random Perturbations of Fourier Modes Representing Coil Distortion Errors plus Random Assembly Errors									
All Coils	3/5	6/10	3/6	6/12	3/7	6/14	1/2	2/4	Totals*
Max	5.2%	1.1%	2.1%	0.2%	0.4%	0.0%	13.8%	4.3%	17.8%
Min	0.4%	0.2%	0.1%	0.0%	0.0%	0.0%	1.3%	0.4%	3.8%
Avg	3.1%	0.7%	1.2%	0.1%	0.2%	0.0%	8.4%	2.6%	11.6%
Stdev	0.9%	0.2%	0.3%	0.0%	0.1%	0.0%	2.4%	0.7%	2.5%

Island Size scales with (tolerance)^{0.5}
Island Size at 1.5 mm is 86.6% of 2 mm tolerance

*Total Flux lost to Islands
Obtained by summing dominant mode from each surface

m=2 mode still most significant, followed by m=5

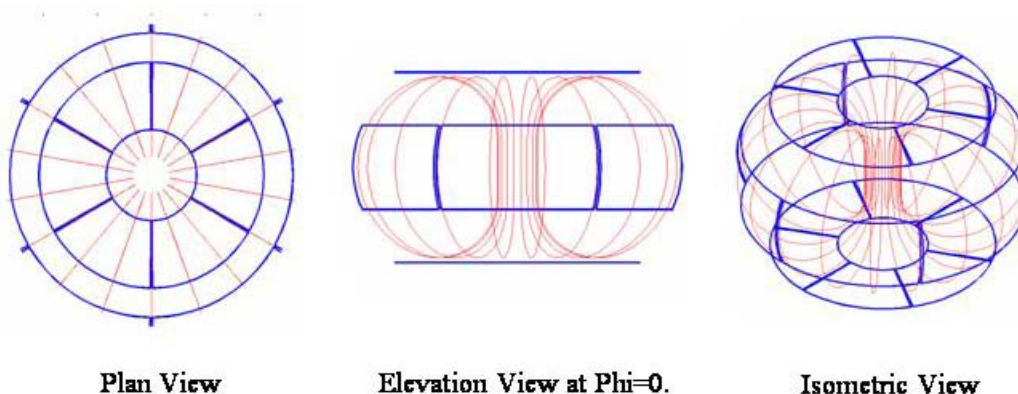
Frequency of Islands for Random Combination of Tolerances



Mitigating Islands with Trim Coils

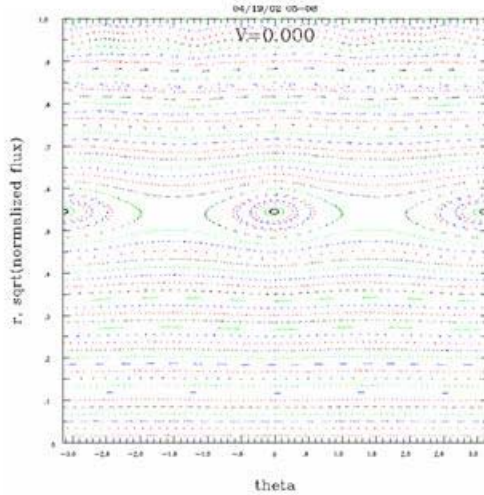
- A set of correction coils (ex-vessel trim coils) was proposed by Hutch Neilson to target low order modes:
 - Outside the TF coils
 - Similar to those found on or proposed for Tokamaks (DIII-D?)
 - 6 horizontal pie sector coils top and bottom
 - 6 large window pane coils outboard
- In-Vessel Trim Coils can be used for symmetric errors ($m=5$, $m=6$)
- Correction coils currents set by SVD targeting low order resonances introduced by field coil errors

Correction Coil Configuration

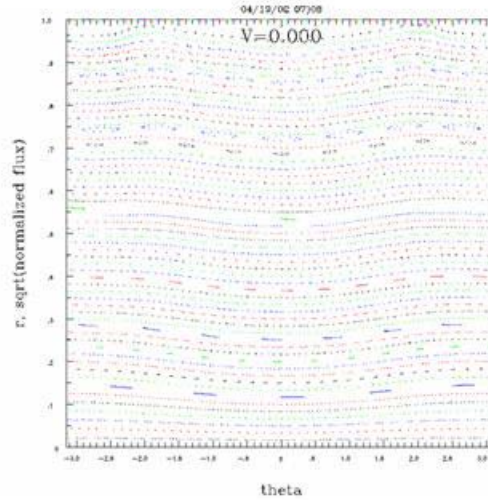


Correction Coils (blue) on TF Coils (red)

Correction Coils Suppressing Symmetric $m=2$ Island



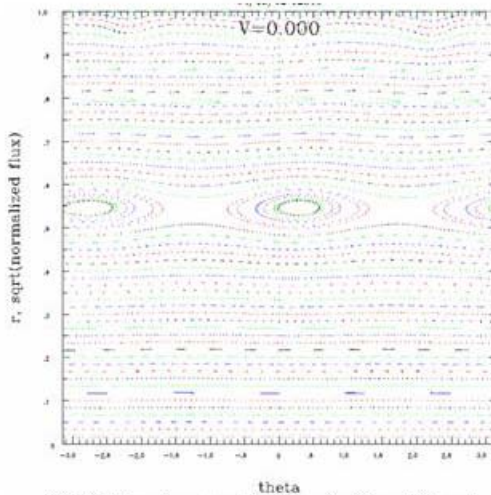
M=2 Symmetric Islands from Worst Case (Modular Coil 1) Distortion



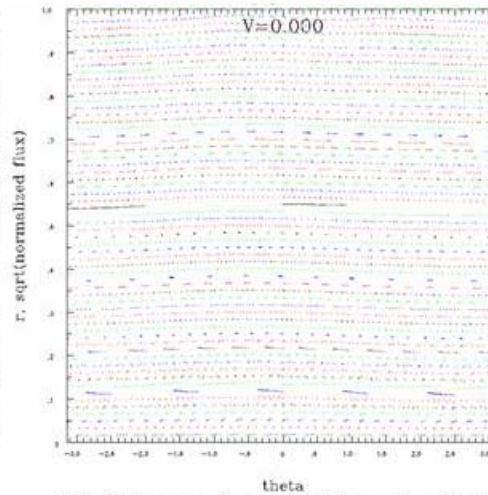
Island Suppression Using Correction Coils

Max Correction Coil Current = 63 KAT

Correction Coils Suppressing Non-Symmetric $m=2$ Island



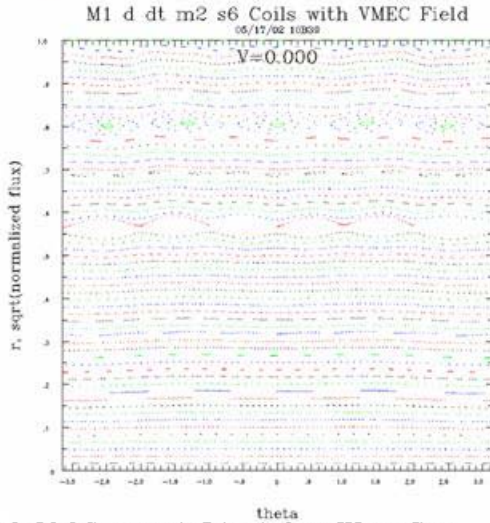
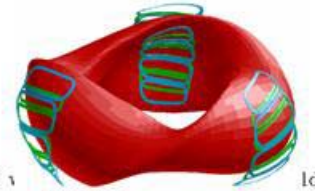
M=2 Non-Symmetric Islands from Worst Case (Modular Coil 3) Distortion



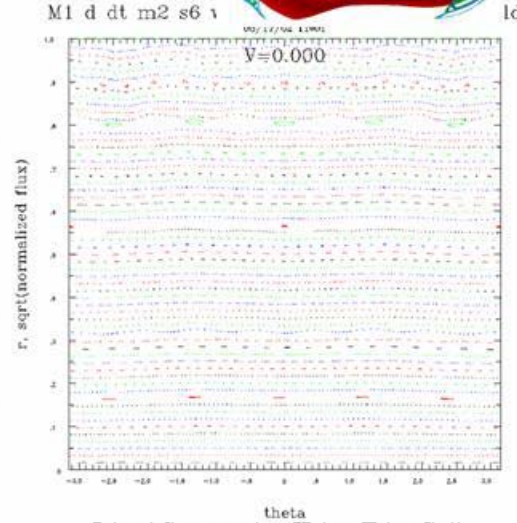
Island Suppression Using Correction Coils

Max Correction Coil Current = 24 KAT

In-Vessel Trim Coils Suppressing Symmetric $m=5$ & $m=6$ Islands



M=5&6 Symmetric Islands from Worst Case (Modular Coil 1) Systematic Distortion with 6 Images



Island Suppression Using Trim Coils

Max Trim Coil Current = 179 AT

Suppressing Islands - Results

Resonance	Island Size, %Flux			
	Single Modular		With 6 Images	
	Before	After	Before	After
1/2	13.6%	0.0%	0.0%	0.0%
2/4	4.1%	0.0%	0.0%	0.0%
3/5	2.8%	0.2%	7.8%	0.0%
6/10	0.8%	0.4%	2.4%	3.4%
3/6	1.8%	0.5%	5.1%	0.0%
6/12	0.2%	0.1%	0.5%	0.8%
3/7	0.2%	0.4%	0.5%	0.9%
Total*	16.5%	1.3%	13.4%	5.1%

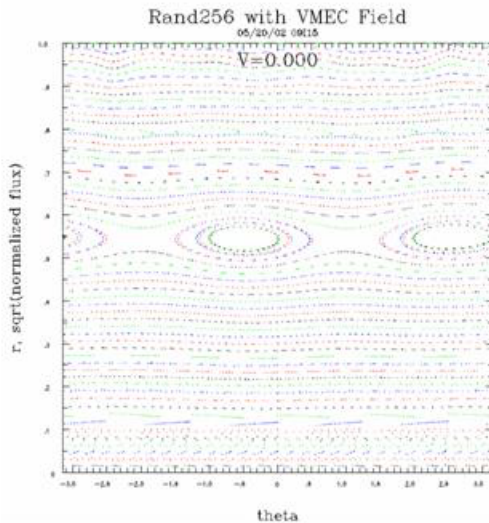
Based on 1.5 mm tolerance
 *Total is sum of dominate modes on each surface

6/10 Island
Excited by
M6 Trim Coil

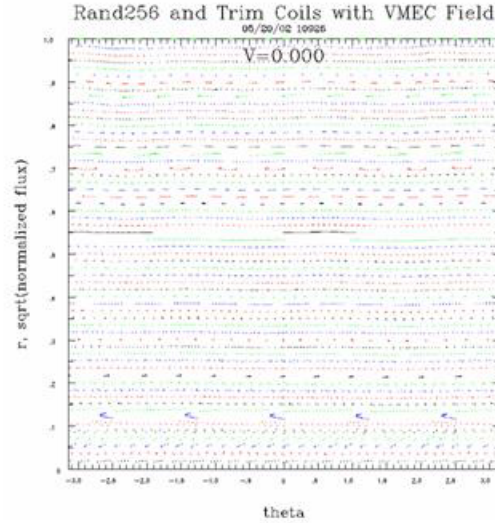
Ex-Vessel
Trim Coils

In-Vessel
Trim Coils

Suppressing Islands for (Nearly) Worst Case Random Stack-up of Tolerance 1.5 mm max



M=2 and Small m=5 Islands from Worst Case Random Stack-up



Island Suppression Using Mainly External Trim Coils

Max Correction Coil Current = 11.7 KAT

Suppressing Islands for (Nearly) Worst Case Random Stack-up of Tolerance 1.5 mm max

Resonance	Island Size, %Flux	
	Before	After
1/2	13.00%	0.00%
2/4	2.50%	0.00%
3/5	3.40%	0.00%
6/10	0.70%	0.90%
3/6	1.30%	0.50%
6/12	0.10%	0.10%
3/7	0.20%	0.20%
Total*	16.60%	1.60%

Based on 1.5 mm tolerance

*Total is sum of dominate modes on each surface

Summary

- Tools are benchmarked and working to assess impact of coil tolerances on field errors
- Errors in Modular Coils have a much larger impact on field errors than do errors in TF or PF coils
- Systematic Perturbation of All Modular Coils is not much worse than a single coil (but they excite different modes)
- Random Perturbation of Fourier Coefficients appears to be only slightly worse
- Correction Coils shown to be effective with low order modes.
- In-vessel trim coils effective against symmetric errors

Back-up Slides
(to CDR Presentation)

Systematic Errors imposed on M45 Modular and TF Coil Assemblies

- Coil Distortions Errors (2 mm max, $m=0..6$)
 - Impose distortions of each modular coil of form:
 - $dR = 0.002 * \sin(m*th)$
 - $dZ = 0.002 * \sin(m*th)$
 - $dPHI = 0.002 * \sin(m*th)$
 - Repeat for cosine distribution
- Coil Assembly Errors (2 mm max, $n=0..6$)
 - Displace or Rotate each modular coil about it's centroid:
 - $dR = 0.002 * \sin(n*phi)$
 - $dZ = 0.002 * \sin(n*phi)$
 - $dPHI = 0.002 * \sin(n*phi)$
 - $Rot_R = 0.002 * \sin(n*phi)$
 - $Rot_Z = 0.002 * \sin(n*phi)$
 - $Rot_PHI = 0.002 * \sin(n*phi)$
 - Repeat for cosine distribution

Note: Distortion Errors and Assembly Errors were investigated separately

Sampling of Results for Systematic Errors imposed on Modular Assemblies

phase	mode	dof	coils	5,3	10,6	6,3	12,6	7,3	14,6	2,1	4,2
cos	0	dr	m45	6.1%	0.6%	2.0%	0.2%	0.4%	0.0%	0.0%	0.0%
cos	1	dr	m45	5.2%	1.3%	2.6%	0.2%	0.1%	0.0%	0.0%	0.0%
cos	2	dr	m45	7.5%	1.9%	3.4%	0.4%	0.1%	0.0%	0.1%	0.0%
cos	3	dr	m45	7.2%	2.1%	3.5%	0.5%	0.4%	0.0%	0.1%	0.0%
cos	4	dr	m45	9.3%	2.1%	3.3%	0.5%	0.6%	0.0%	0.1%	0.0%
cos	5	dr	m45	6.6%	1.8%	2.2%	0.4%	0.5%	0.0%	0.1%	0.0%
cos	6	dr	m45	8.6%	0.4%	2.7%	0.3%	0.3%	0.0%	0.1%	0.0%
cos	0	dz	m45	5.8%	1.7%	1.8%	0.4%	0.7%	0.0%	0.0%	0.0%
cos	1	dz	m45	5.8%	1.8%	2.3%	0.3%	0.5%	0.0%	0.0%	0.0%
cos	2	dz	m45	6.2%	1.9%	3.1%	0.4%	0.5%	0.0%	0.0%	0.0%
cos	3	dz	m45	6.1%	1.8%	3.5%	0.4%	0.5%	0.0%	0.0%	0.0%
cos	4	dz	m45	6.6%	2.0%	3.7%	0.5%	0.4%	0.0%	0.0%	0.0%
cos	5	dz	m45	7.0%	2.0%	3.0%	0.4%	0.3%	0.0%	0.0%	0.0%
cos	6	dz	m45	7.6%	1.1%	2.1%	0.3%	0.3%	0.0%	0.0%	0.0%
cos	0	dt	m45	5.1%	1.2%	1.4%	0.2%	0.5%	0.0%	0.1%	0.0%
cos	1	dt	m45	6.9%	1.9%	3.0%	0.4%	0.6%	0.0%	0.1%	0.0%
cos	2	dt	m45	7.1%	1.3%	3.8%	0.4%	0.4%	0.0%	0.1%	0.0%
cos	3	dt	m45	13.4%	2.4%	4.9%	0.6%	0.3%	0.0%	0.1%	0.0%
cos	4	dt	m45	11.0%	2.9%	4.9%	0.6%	0.5%	0.0%	0.1%	0.0%
cos	5	dt	m45	3.4%	2.6%	3.4%	0.6%	0.4%	0.0%	0.1%	0.0%
cos	6	dt	m45	6.2%	1.2%	2.4%	0.5%	0.3%	0.0%	0.1%	0.0%

Each Modular Coil *Distorted* $.002 \cos(m\theta)$

Sampling of Results for Systematic Errors imposed on Modular Assemblies

phase	mode	dof	c.coils	5,3	10,6	6,3	12,6	7,3	14,6	2,1	4,2
cos	0	dr	m45	0.1%	0.6%	2.0%	0.2%	0.4%	0.0%	0.0%	0.0%
cos	1	dr	m45	0.2%	0.1%	0.1%	0.0%	0.0%	0.0%	6.0%	4.5%
cos	2	dr	m45	0.2%	0.1%	0.1%	0.0%	0.0%	0.0%	10.9%	1.3%
cos	3	dr	m45	4.0%	1.4%	2.7%	0.2%	0.1%	0.0%	0.0%	0.0%
cos	4	dr	m45	0.2%	0.1%	0.1%	0.0%	0.0%	0.0%	5.1%	5.3%
cos	5	dr	m45	0.2%	0.1%	0.1%	0.0%	0.0%	0.0%	12.7%	2.0%
cos	6	dr	m45	1.9%	1.5%	2.2%	0.2%	0.2%	0.0%	0.0%	0.0%
cos	0	dz	m45	5.8%	1.7%	1.8%	0.4%	0.7%	0.0%	0.0%	0.0%
cos	1	dz	m45	0.2%	0.1%	0.1%	0.0%	0.0%	0.0%	12.1%	5.6%
cos	2	dz	m45	0.2%	0.1%	0.1%	0.0%	0.0%	0.0%	18.7%	3.0%
cos	3	dz	m45	7.0%	1.6%	2.7%	0.3%	0.3%	0.0%	0.0%	0.0%
cos	4	dz	m45	0.2%	0.1%	0.1%	0.0%	0.0%	0.0%	8.5%	5.5%
cos	5	dz	m45	0.2%	0.1%	0.1%	0.0%	0.0%	0.0%	12.3%	1.8%
cos	6	dz	m45	1.8%	1.4%	2.2%	0.2%	0.1%	0.0%	0.0%	0.0%
cos	0	dt	m45	5.1%	1.2%	1.4%	0.2%	0.5%	0.0%	0.1%	0.0%
cos	1	dt	m45	0.1%	0.0%	0.0%	0.0%	0.0%	0.0%	6.1%	1.8%
cos	2	dt	m45	0.1%	0.0%	0.0%	0.0%	0.0%	0.0%	11.9%	1.4%
cos	3	dt	m45	1.0%	0.8%	1.0%	0.2%	0.3%	0.0%	0.1%	0.0%
cos	4	dt	m45	0.1%	0.0%	0.0%	0.0%	0.0%	0.0%	6.4%	0.9%
cos	5	dt	m45	0.1%	0.0%	0.0%	0.0%	0.0%	0.0%	8.4%	2.0%
cos	6	dt	m45	3.7%	0.6%	0.9%	0.1%	0.1%	0.0%	0.1%	0.0%

Each Modular Coil *Displaced* by .002 cos(mφ)

Systematic Errors imposed on Individual M45 Modular and TF Coils

- Coil Distortions Errors (2 mm max, m=0..6)
 - Impose distortions of each modular coil of form:
 - $dR = 0.002 * \sin(m*th)$
 - $dZ = 0.002 * \sin(m*th)$
 - $dPHI = 0.002 * \sin(m*th)$
 - Repeat for cosine distribution
- Coil Assembly Errors (2 mm max, n=0..6)
 - Displace or Rotate each modular coil about it's centroid:
 - $dR = 0.002$
 - $dZ = 0.002$
 - $dPHI = 0.002$
 - $Rot_R = 0.002$
 - $Rot_Z = 0.002$
 - $Rot_PHI = 0.002$

Notes: Distortion Errors
and Assembly Errors
were investigated separately

Sampling of Results for Systematic Errors imposed on Individual Modular Coils

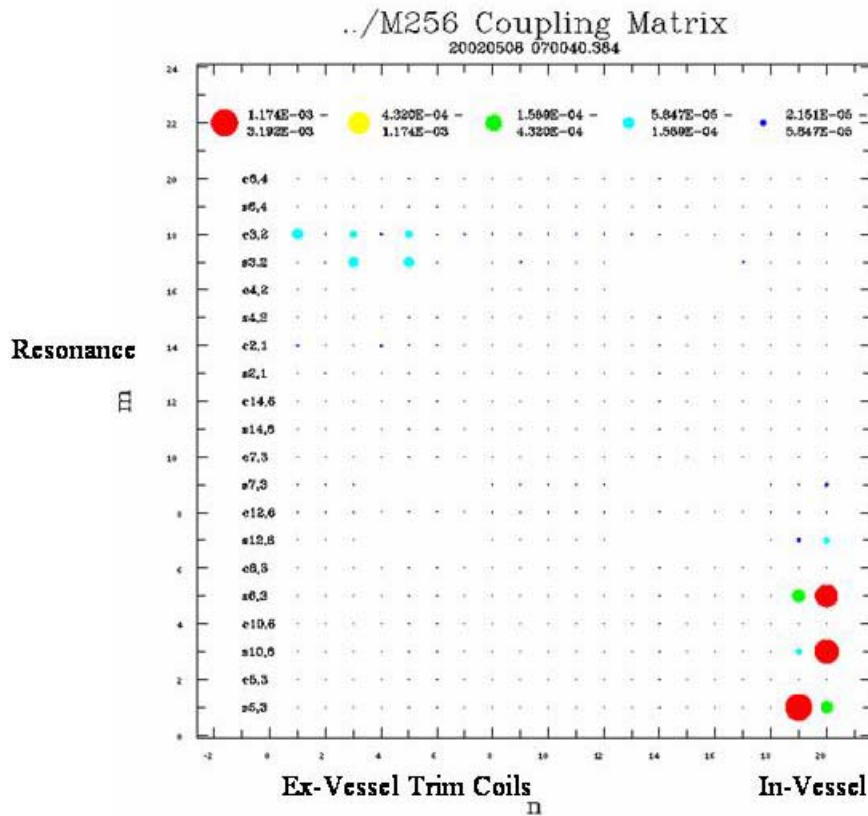
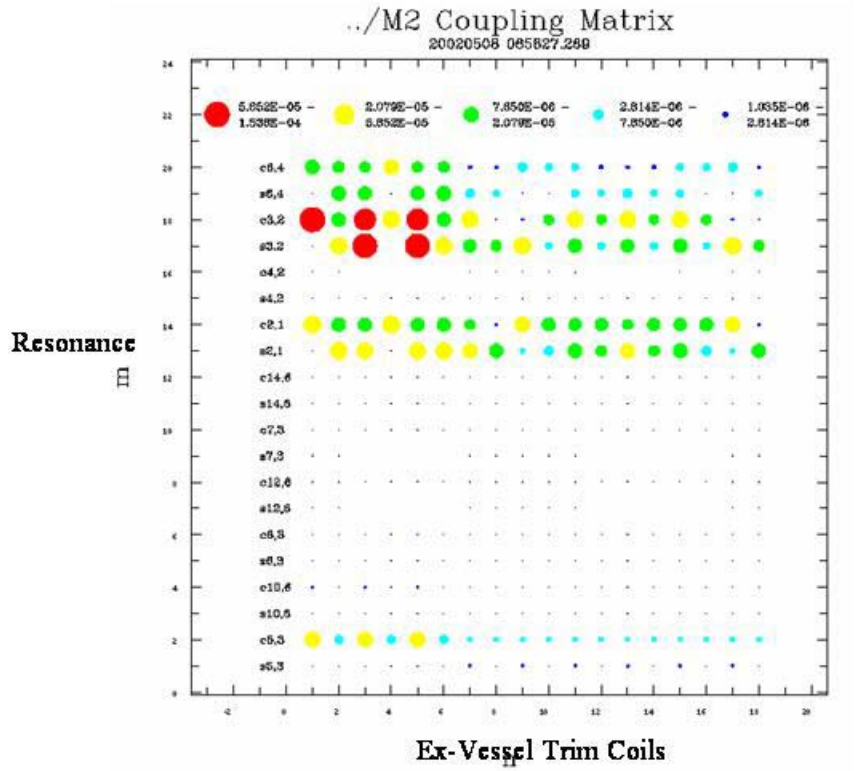
phase	mode	dof	coils	5,3	10,6	6,3	12,6	7,3	14,6	2,1	4,2
sin	0	dr	m1	0.0%	0.0%	0.0%	0.0%	0.0%	0.0%	0.0%	0.0%
sin	1	dr	m1	1.8%	0.6%	0.9%	0.1%	0.1%	0.0%	5.5%	2.2%
sin	2	dr	m1	2.8%	0.8%	1.3%	0.2%	0.2%	0.0%	6.5%	2.9%
sin	3	dr	m1	2.1%	0.9%	1.3%	0.2%	0.2%	0.0%	5.9%	2.8%
sin	4	dr	m1	2.2%	0.8%	1.1%	0.2%	0.2%	0.0%	4.2%	2.1%
sin	5	dr	m1	1.5%	0.7%	1.0%	0.2%	0.2%	0.0%	5.3%	2.1%
sin	6	dr	m1	1.8%	0.5%	0.7%	0.2%	0.2%	0.0%	5.7%	2.4%
sin	0	dz	m1	0.0%	0.0%	0.0%	0.0%	0.0%	0.0%	0.0%	0.0%
sin	1	dz	m1	1.9%	0.6%	1.1%	0.1%	0.1%	0.0%	6.4%	2.2%
sin	2	dz	m1	1.9%	0.8%	1.4%	0.2%	0.1%	0.0%	7.2%	2.8%
sin	3	dz	m1	2.2%	0.8%	1.3%	0.2%	0.1%	0.0%	6.2%	2.6%
sin	4	dz	m1	1.9%	0.7%	0.9%	0.2%	0.2%	0.0%	5.4%	1.7%
sin	5	dz	m1	1.4%	0.6%	0.8%	0.2%	0.2%	0.0%	6.6%	1.7%
sin	6	dz	m1	1.9%	0.6%	0.9%	0.1%	0.1%	0.0%	4.6%	2.3%
sin	0	dt	m1	0.0%	0.0%	0.0%	0.0%	0.0%	0.0%	0.0%	0.0%
sin	1	dt	m1	2.5%	0.7%	1.5%	0.1%	0.2%	0.0%	8.5%	3.4%
sin	2	dt	m1	3.2%	1.0%	2.1%	0.2%	0.2%	0.0%	15.7%	4.7%
sin	3	dt	m1	4.4%	1.1%	2.0%	0.2%	0.1%	0.0%	10.2%	3.8%
sin	4	dt	m1	3.0%	1.2%	2.0%	0.2%	0.2%	0.0%	2.6%	4.1%
sin	5	dt	m1	3.2%	1.0%	1.4%	0.3%	0.2%	0.0%	6.7%	2.3%
sin	6	dt	m1	1.2%	0.9%	0.9%	0.2%	0.2%	0.0%	9.9%	2.9%

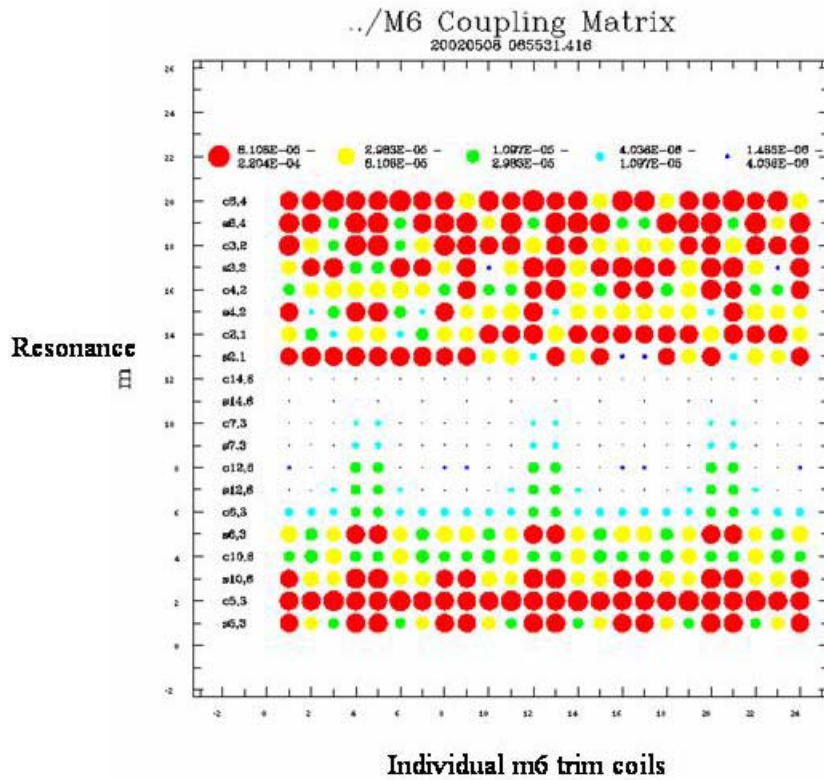
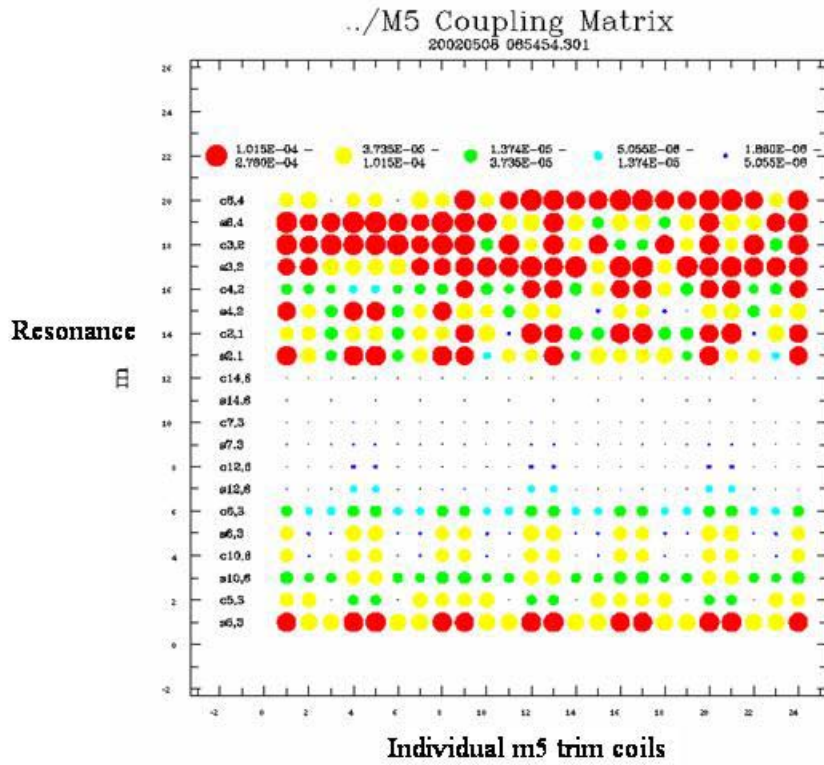
Modular Coil 1 (single coil) *Distorted* .002 sin(mθ)

Sampling of Results for Systematic Errors imposed on Individual TF Coils

phase	mode	dof	coils	5,3	10,6	6,3	12,6	7,3	14,6	2,1	4,2
sin	0	dr	tf1	0.0%	0.0%	0.0%	0.0%	0.0%	0.0%	0.0%	0.0%
sin	1	dr	tf1	0.2%	0.0%	0.1%	0.0%	0.0%	0.0%	1.3%	0.3%
sin	2	dr	tf1	0.4%	0.1%	0.1%	0.0%	0.0%	0.0%	1.2%	0.4%
sin	3	dr	tf1	0.4%	0.1%	0.1%	0.0%	0.0%	0.0%	1.5%	0.3%
sin	4	dr	tf1	0.3%	0.1%	0.1%	0.0%	0.0%	0.0%	1.3%	0.3%
sin	5	dr	tf1	0.3%	0.1%	0.1%	0.0%	0.0%	0.0%	0.9%	0.2%
sin	6	dr	tf1	0.2%	0.0%	0.1%	0.0%	0.0%	0.0%	0.6%	0.2%
sin	0	dz	tf1	0.0%	0.0%	0.0%	0.0%	0.0%	0.0%	0.0%	0.0%
sin	1	dz	tf1	0.2%	0.0%	0.1%	0.0%	0.0%	0.0%	1.7%	0.2%
sin	2	dz	tf1	0.2%	0.1%	0.0%	0.0%	0.0%	0.0%	1.3%	0.3%
sin	3	dz	tf1	0.1%	0.1%	0.1%	0.0%	0.0%	0.0%	1.2%	0.2%
sin	4	dz	tf1	0.3%	0.0%	0.1%	0.0%	0.0%	0.0%	0.9%	0.3%
sin	5	dz	tf1	0.2%	0.0%	0.0%	0.0%	0.0%	0.0%	0.5%	0.1%
sin	6	dz	tf1	0.1%	0.0%	0.0%	0.0%	0.0%	0.0%	0.2%	0.1%
sin	0	dt	tf1	0.0%	0.0%	0.0%	0.0%	0.0%	0.0%	0.0%	0.0%
sin	1	dt	tf1	0.4%	0.0%	0.2%	0.0%	0.0%	0.0%	2.7%	0.2%
sin	2	dt	tf1	0.5%	0.1%	0.3%	0.0%	0.0%	0.0%	3.1%	0.6%
sin	3	dt	tf1	0.6%	0.1%	0.2%	0.0%	0.0%	0.0%	0.7%	0.7%
sin	4	dt	tf1	0.7%	0.1%	0.2%	0.0%	0.0%	0.0%	1.4%	0.5%
sin	5	dt	tf1	0.2%	0.1%	0.1%	0.0%	0.0%	0.0%	1.1%	0.3%
sin	6	dt	tf1	0.2%	0.1%	0.1%	0.0%	0.0%	0.0%	0.7%	0.2%

TF Coil 1 (single coil) *Distorted* .002 sin(mθ)



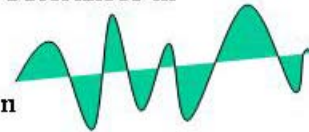


Post CDR Coil Tolerance Studies

Coil Tolerance Studies

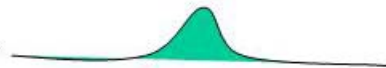
- **Impact of Random Tolerance Stack up for Different Tolerances in Modular, TF and PF**

- Using Fourier Representation (alla CDR)
- Local Tolerance varies with Coil-to-Plasma Separation



- **Impact of short “wavelet” type deformation on Modular Coils**

- Island Size vs Coil-to-Plasma Separation
- In-Plane and Out-of-Plane Deformations
- Modular Coils 1,2 &3 Considered Individually




- **Impact of broad deformations of Modular Coils**

- Island Size vs Closest Coil-to-Plasma Separation
- Out-of-Plane Deformations of Modular Coil 1 Only



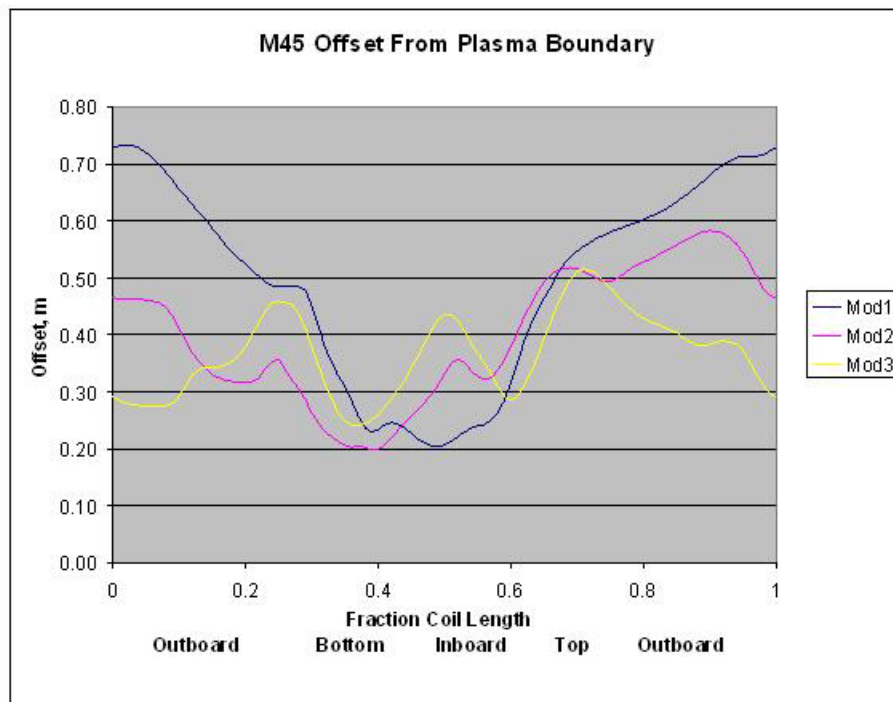
Impact of Tolerance Schemes on Modular, TF and PF

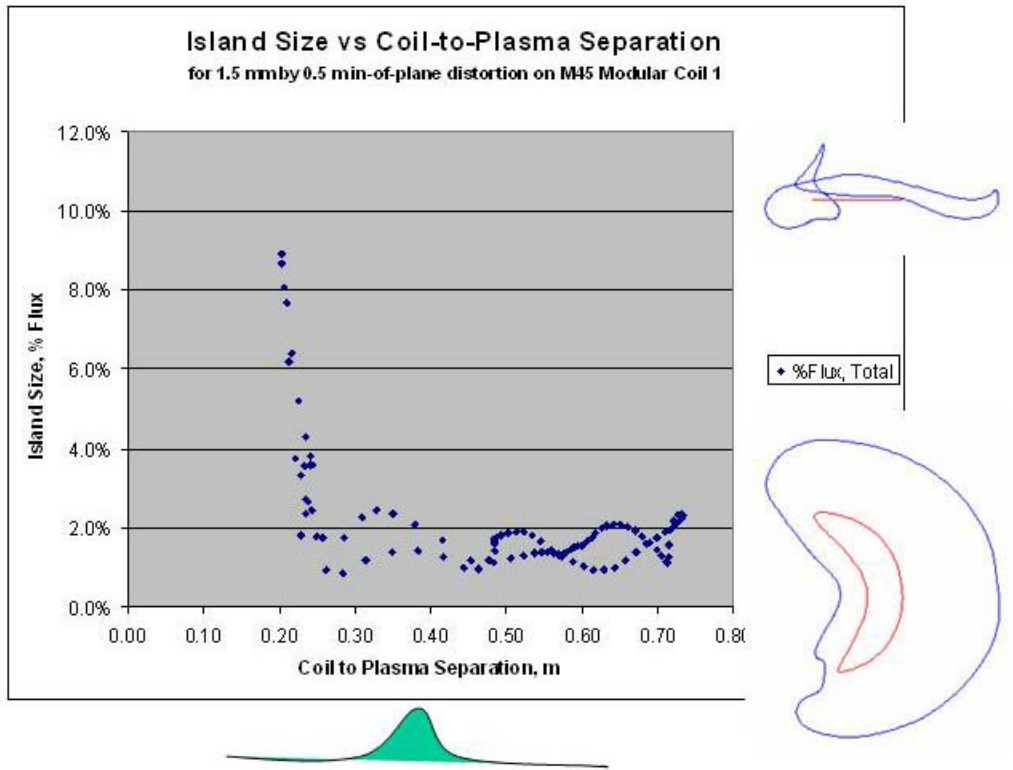
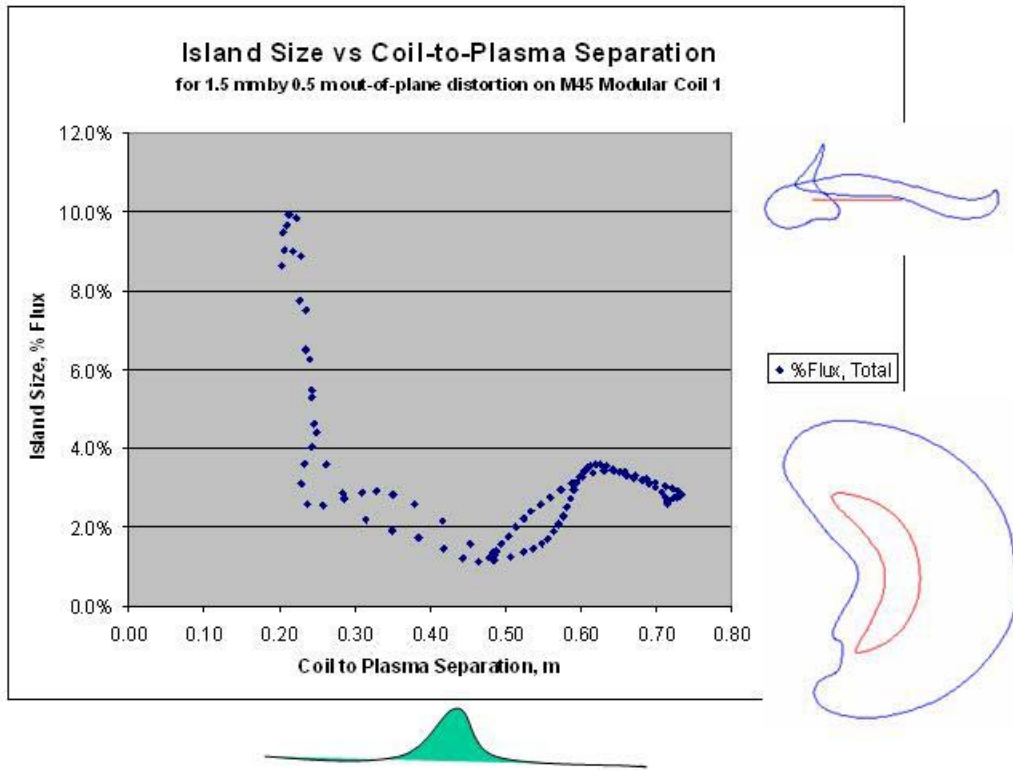
Summary of the Effect of Random Coil Distortions on Island Sizes with Various Tolerance Schemes

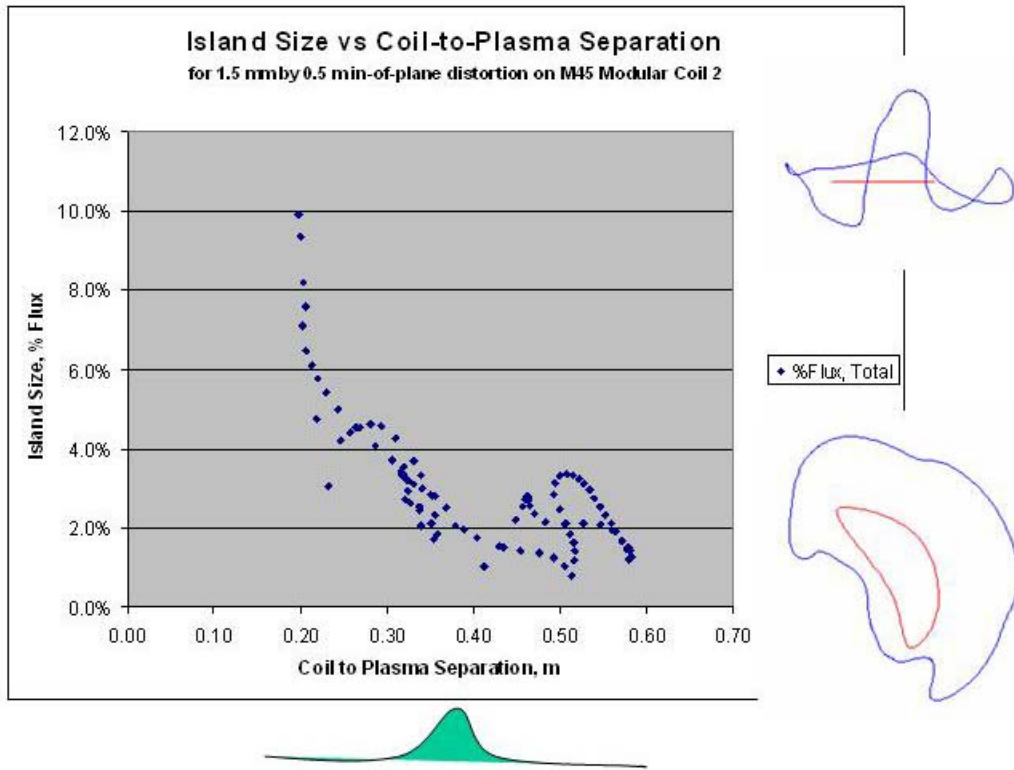
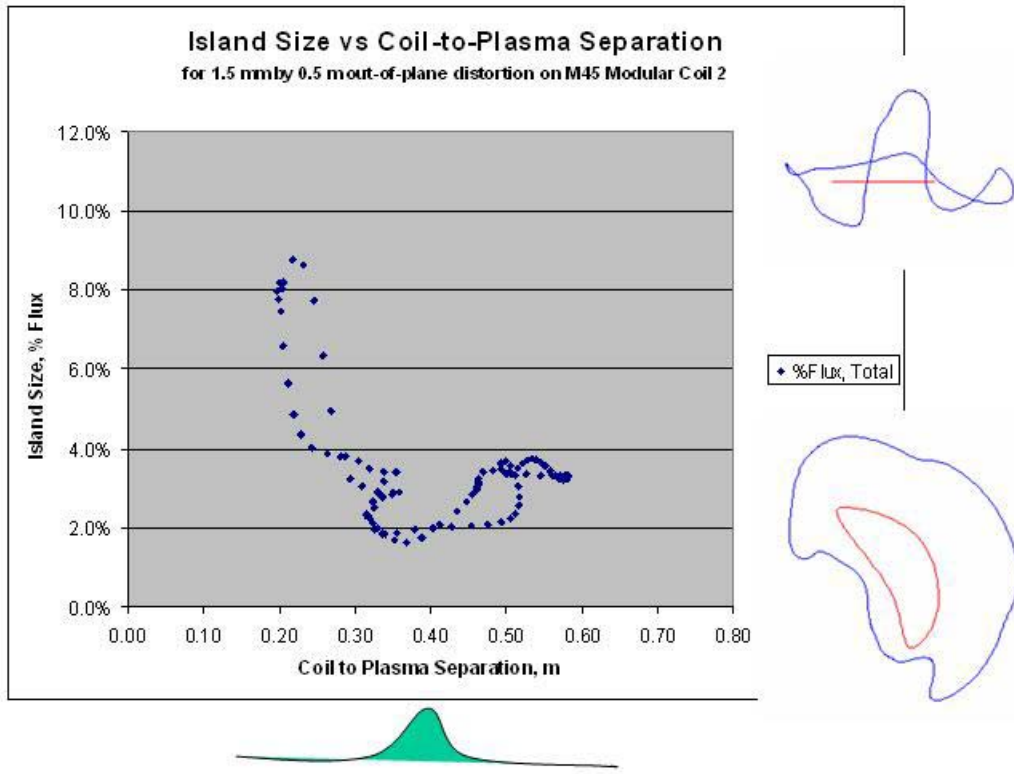


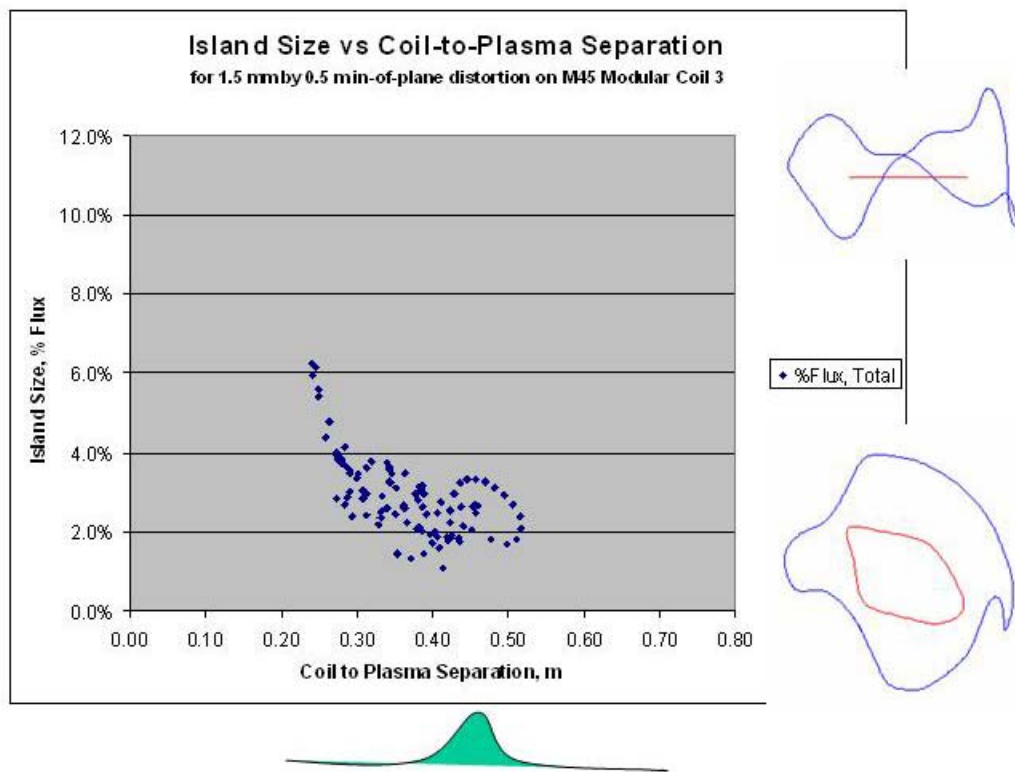
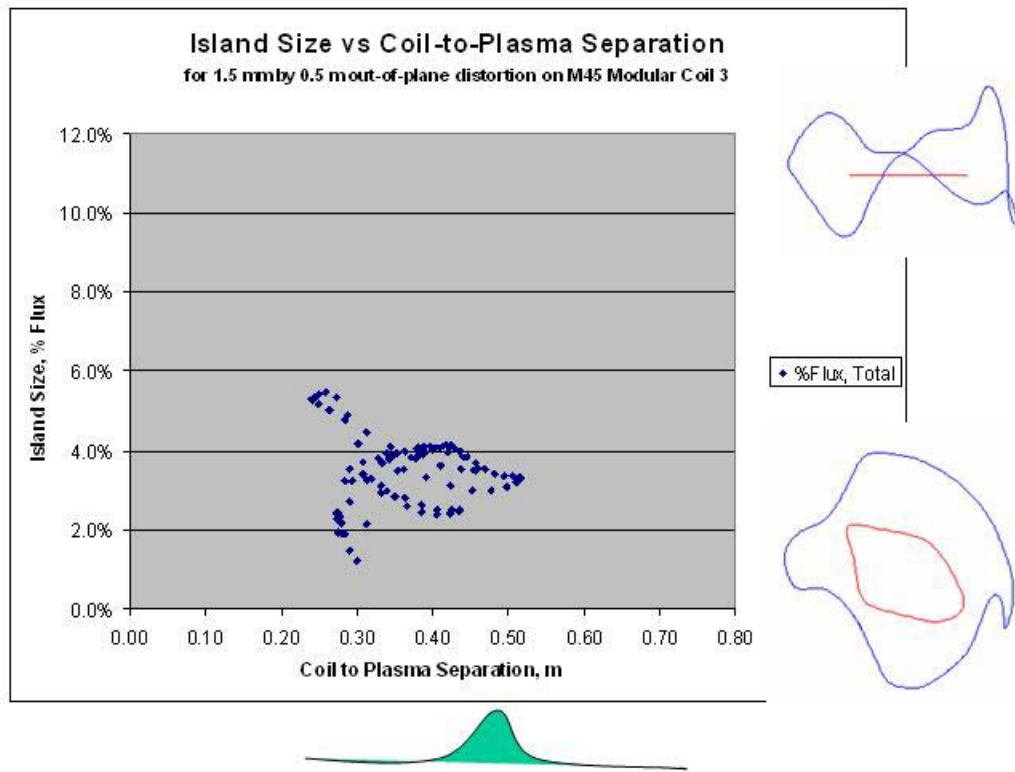
Tolerance	m.m	Resonance	3/5	6/10	3/6	1/2	2/4	Totals	Comments
Modular	1.5	Max	5.2%	1.1%	2.1%	13.8%	4.3%	17.8%	CDR Results Error found in form of distortion
TF	1.5	Min	0.4%	0.2%	0.1%	1.3%	0.4%	3.8%	
PF	1.5	Arg	3.1%	0.7%	1.2%	8.4%	2.6%	11.6%	
		stdev	0.9%	0.2%	0.3%	2.4%	0.7%	2.5%	
Modular	1.5	Max	6.1%	1.4%	2.5%	16.4%	5.1%	22.1%	Corrected
TF	1.5	Min	1.2%	0.2%	0.4%	3.6%	0.9%	7.3%	
PF	1.5	Arg	3.7%	0.8%	1.5%	9.9%	3.2%	13.9%	(and still correctable)
		stdev	1.0%	0.2%	0.4%	2.5%	0.9%	2.6%	
Modular	1.5	Max	6.1%	1.4%	2.5%	16.6%	5.1%	22.2%	TF & PF Tolerance
TF	3.0	Min	1.5%	0.3%	0.4%	3.4%	1.1%	7.1%	Has negligible impact
PF	3.0	Arg	3.7%	0.8%	1.5%	10.0%	3.2%	13.9%	on overall results
		stdev	1.0%	0.2%	0.4%	2.6%	0.8%	2.7%	
Modular	1.5-3.0	Max	6.6%	1.5%	2.5%	19.1%	5.4%	24.3%	Softening Mod Tolerance
TF	3.0	Min	1.1%	0.3%	0.4%	3.0%	1.2%	7.4%	away from plasma
PF	3.0	Arg	3.9%	0.9%	1.5%	11.1%	3.3%	15.2%	has small impact
		stdev	1.0%	0.2%	0.4%	2.8%	0.9%	2.8%	(still correctable)
Modular	3.0	Max	8.7%	2.1%	3.5%	23.2%	7.2%	31.2%	Softening Mod Tolerance
TF	3.0	Min	1.7%	0.3%	0.6%	5.1%	1.2%	10.3%	everywhere
PF	3.0	Arg	5.2%	1.2%	2.1%	14.1%	4.5%	19.6%	has sizeable impact
		stdev	1.4%	0.3%	0.6%	3.6%	1.2%	3.7%	(not correctable)

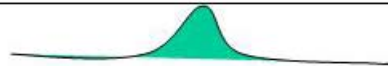
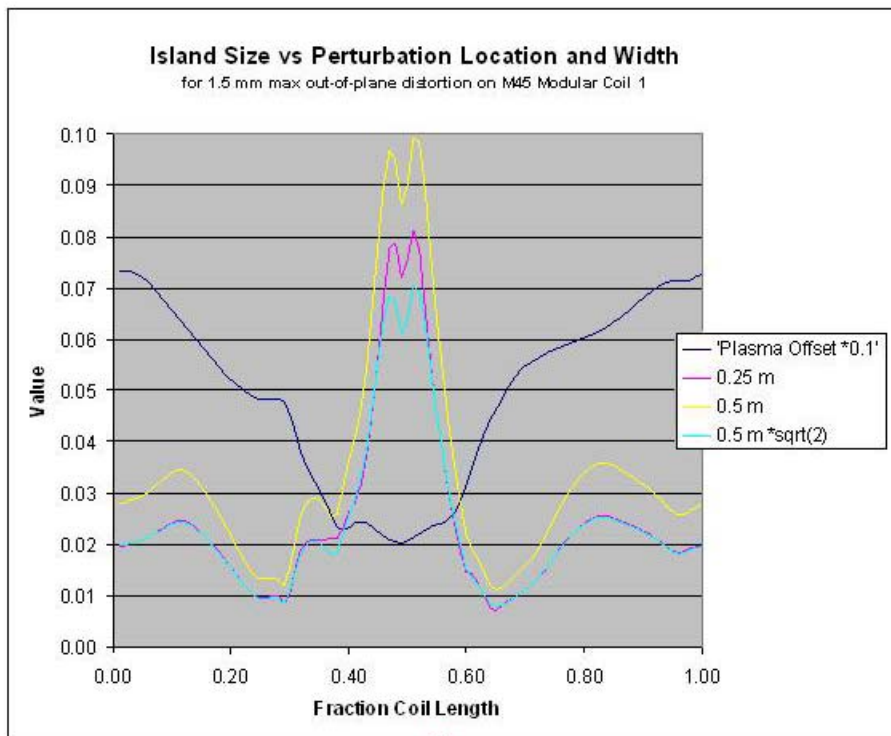
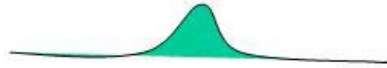
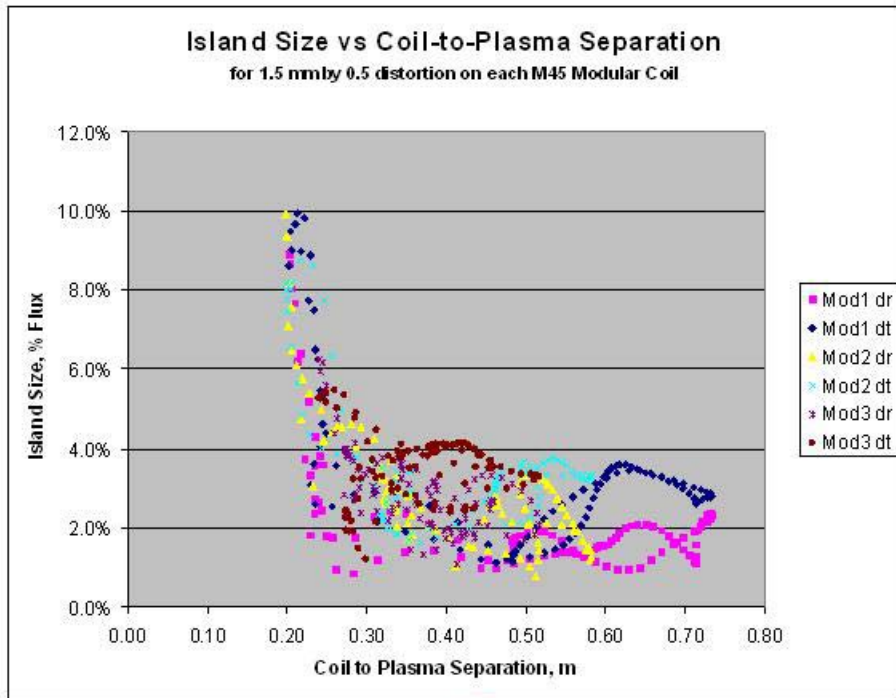
Impact of short “wavelet” type deformation on Modular Coils



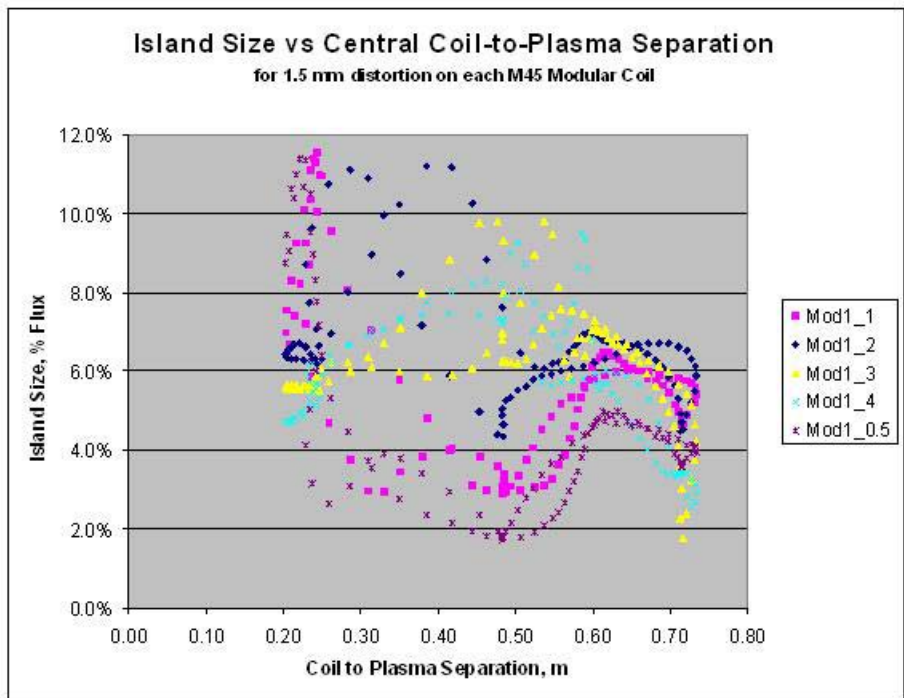
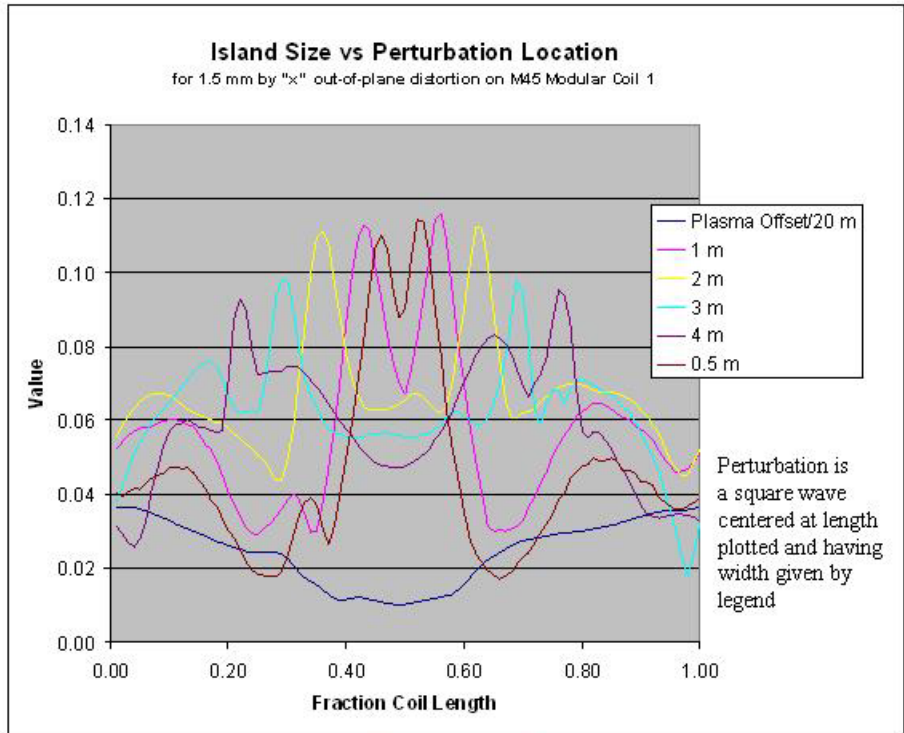


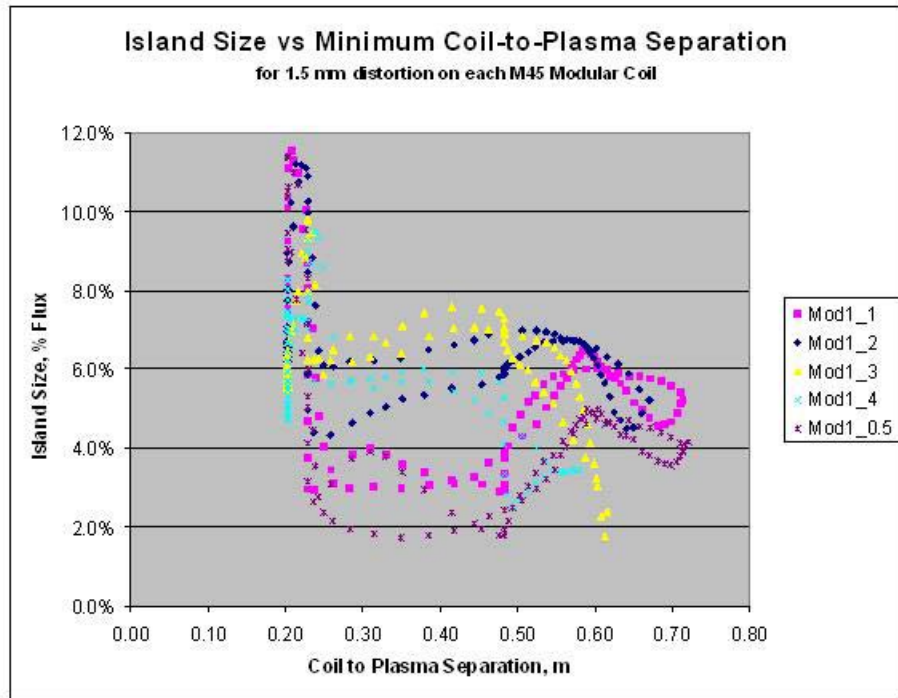






Impact of broad deformations of Modular Coils





Summary

- **Impact of Random Tolerance Stack up for Different Tolerances in Modular, TF and PF**
 - Softening Tolerance on TF & PF from 1.5 to 3.0 mm appears acceptable
 - Softening **Overall** Tolerance on Modulators **not acceptable**.
 - Softening Modular Tolerance based on plasma separation (1.5mm near plasma to 3.0 far from plasma) has minimal impact
- **Impact of short “wavelet” type deformation on Modular Coils**
 - Coil-to-Plasma Separation less than 30 cm has strongest impact on island size
 - In-plane and Out-of-Plane deformations do not differ significantly
- **Impact of broad deformations of Modular Coils**
 - Increasing Length of deformation does not Increase Max Island Size



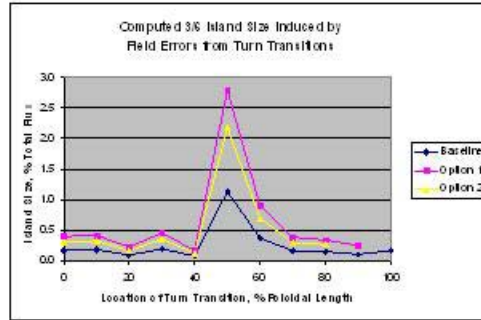
3.1.2 Leads and Turn Transitions

A number of winding options have been considered for the modular coils. These include conventional (one-in-hand) where the conductor winds up one layer and down the adjacent, and multiple-in-hand (2, 3 or the most recent 4) where the multiple turns are treated as a single conductor (ie at the same potential) and all turns raise or fall layer to layer together. The multiple-in-hand options were motivated by the need to reduce keystoneing in the conductor during winding around tight bends by reducing the size of individual conductor turns. However, whereas the one-in-hand option has turn transitions that produce field errors that tend to cancel each other and form smaller current loops, the multiple-in-hand options require an external lead along the side of the bundle to close an effectively larger current loop with potential larger field errors.

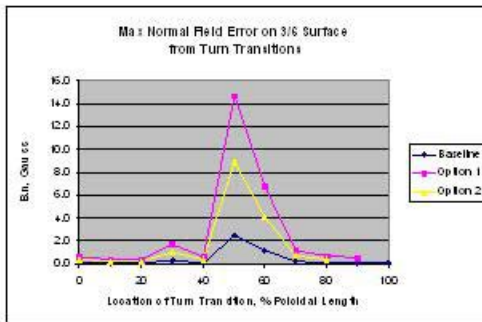
Field errors from each configuration option were compared by calculating the differential field from each configuration and an idealized, no transition (i.e. parallel, nested turns) configuration. By subtracting the configurations themselves as opposed the field from each configuration separately, results in computationally a smaller, identical problem. Several different approaches were taken to model these equivalent configurations. Initially, the length of transition was ignored and the options were compared based on equivalent planar loops normal to the winding direction. A refinement to this inclined the loops to try and account the length of the transition. Finally, a detailed model of the individual turn transitions was made (ie the 'basket' model) which reflected the difference between the actually winding of each configuration, and a multifilament winding of parallel conductors.

The poloidal location of the turn transition and accompanying lead stems was varied as we looked at field errors and induced islands from each configuration. The figures that follow further describe the configurations and the results obtained. Results indicate preferred locations for the turn transition to minimize field errors and island sizes.

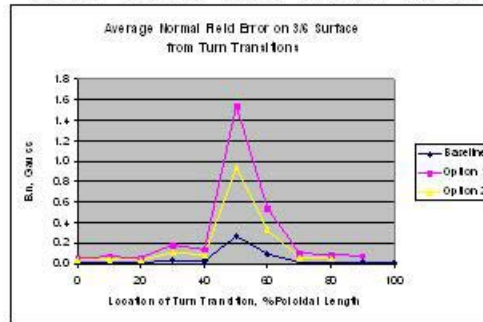
3/6 Field Errors on M50 Plasma from Turn Transition Options vs Poloidal Location



Outboard – Top/Bottom – Inboard – Bottom/top - Outboard



Outboard – Top/Bottom – Inboard – Bottom/top - Outboard



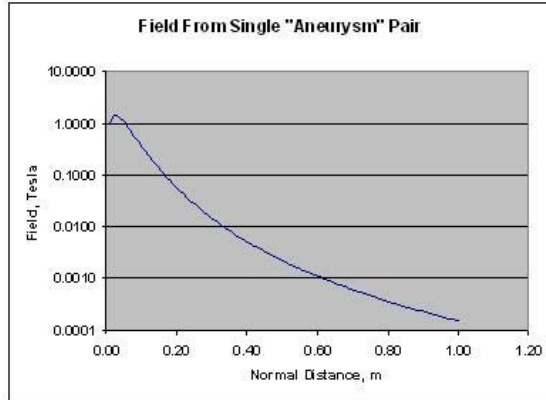
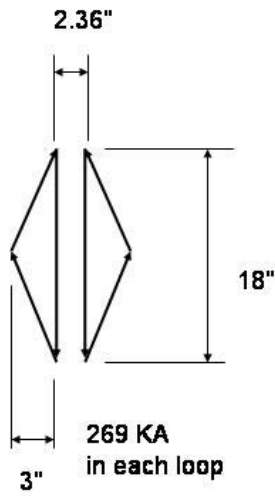
Outboard – Top/Bottom – Inboard – Bottom/top - Outboard

3.1.3 Modular Leads

One option under consideration for returning the modular coil leads was to spread the windings apart on either side of the T support structure, leaving room for a hole in the structure to route the leads. This perturbation to the winding geometry produces current loops with respect to the original geometry. That is to say the difference in the winding geometry of the perturbed on unperturbed coil can be modeled as two equivalent loops with opposite current direction as shown in the sketches below. Field errors from these loops were evaluated as described in Section 2.

The poloidal location of the aneurysm on the modular coils was varied. The results, plotted below, show the field errors and the predicted island size for each location. The unacceptably high field errors and large islands led to the abandoning this approach.

Field Error from "Aneurysm" in Modular Coil formed by Spreading Windings to Accommodate Leads

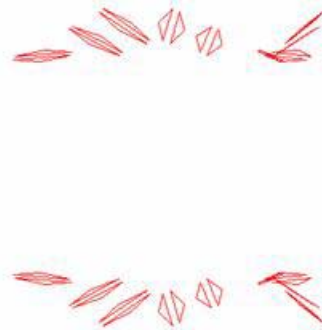


Simplified Equivalent Current Loop

Equivalent Loops for All Modular Coils Shown at Poloidal Location ~ 75% Length from Outboard Midplane

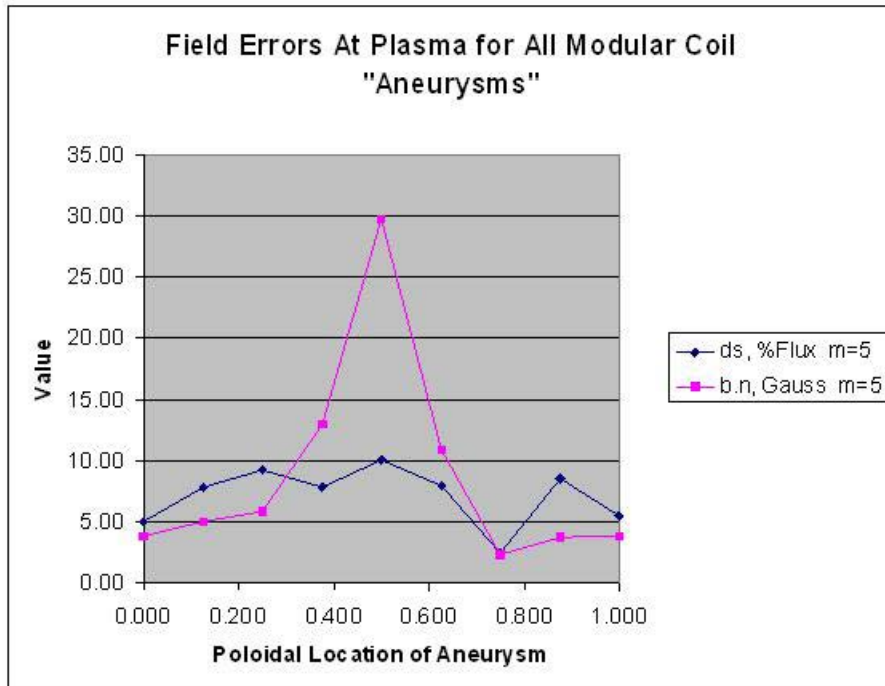
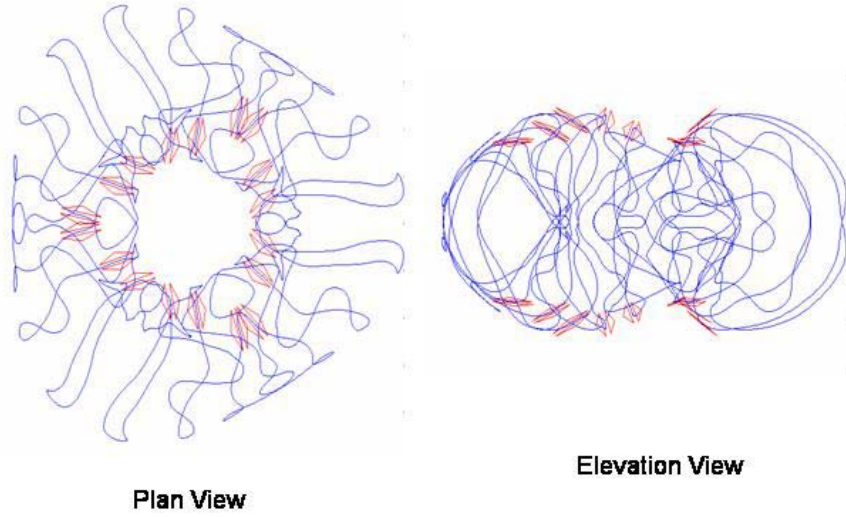


Plan View



Elevation View

Equivalent Loops for All Modular Coils
Shown at Poloidal Location ~ 75% Length from Outboard Midplane and Relative to Modular Coils



3.2 EDDY CURRENTS

3.2.1 Modular Coil Support Structure

The modular coil support structure (or shell) was designed to minimize the impact of eddy currents on field errors and plasma operation. By including electrical insulation between each coil support within a field period and possibly between field periods to break up toroidal current loops and adding a poloidal break the time constant is less than the 20 ms required. Without the poloidal break, the time constant would be significantly larger (~70 ms), violating the 20 ms requirement. Since inclusion of the poloidal break represented a significant impact on the design and fabrication of the modular coil support, an assessment was made of the field errors that would be present without the poloidal break.

The SPARK model used to determine the time constants of the structures was run through a transient where it was excited by the 1.7 T High Beta scenario. This scenario chosen since it produced the largest rate of change of effective dipole moment for the PF coil system, the dominant source of remote field. Searching for the largest eddy currents during the transient (as an indicator of largest field errors) revealed the end of modular coil current ramp-up to be the most severe, but as this is before plasma initiation, it is not of concern. The time of the next largest eddy current loops, the start of flattop, is of concern. Field errors resulting from these eddy currents without a poloidal break are fairly large (~ 16 % flux in islands) and deemed unacceptable. For comparison, the field errors with the poloidal break produce islands that are half as big (which is still significant), but since the time constant is less than 20 ms, they are considered tolerable.

Modular Coil Shell Segmentation Study Field Errors and Time Constants

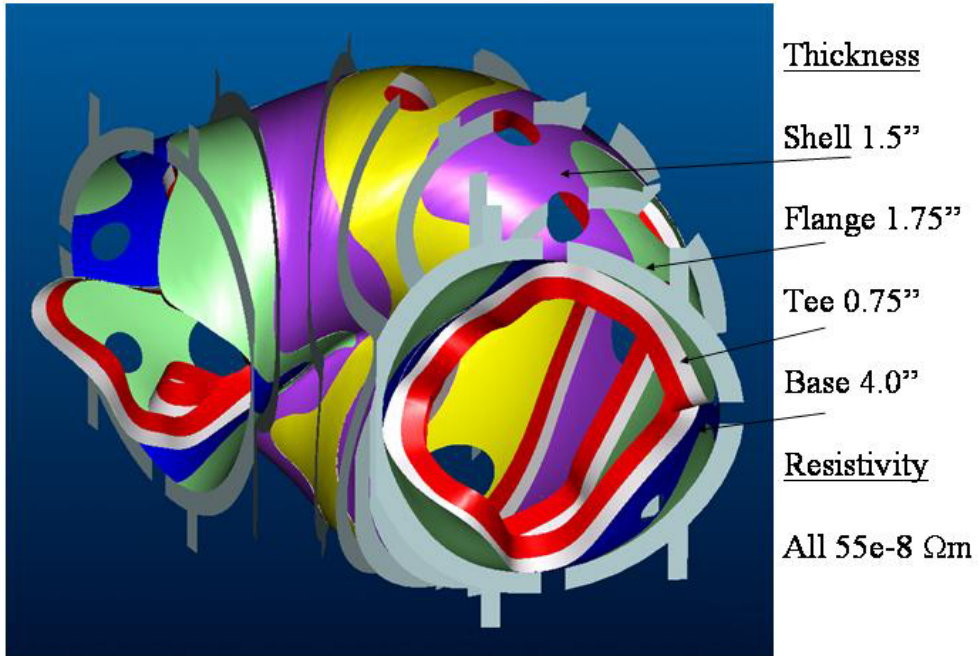
NCSX Engineering Meeting
February 12, 2003

Art Brooks

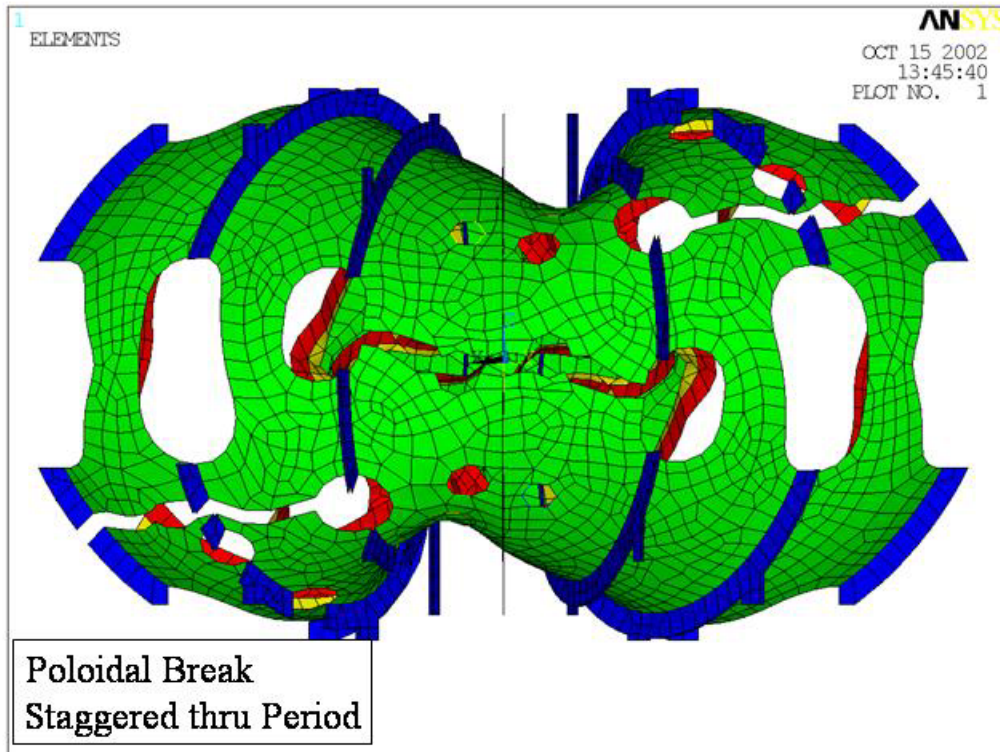
Overview

- Previous examination of Eddy Currents in Modular Coil Shell focused on Time Constants Only
 - Stated requirement was for longest time constant to be less than 20 ms
 - Poloidal Break required to meet this
 - ~70 ms w/o break vs ~16 ms with break
- Question was raised “how bad are resonant error fields if we don’t have poloidal breaks”
 - Consider excitation not during Modular Coil Ramp, but during pulse when toroidal flux from Modular Coils and TF coils is held constant

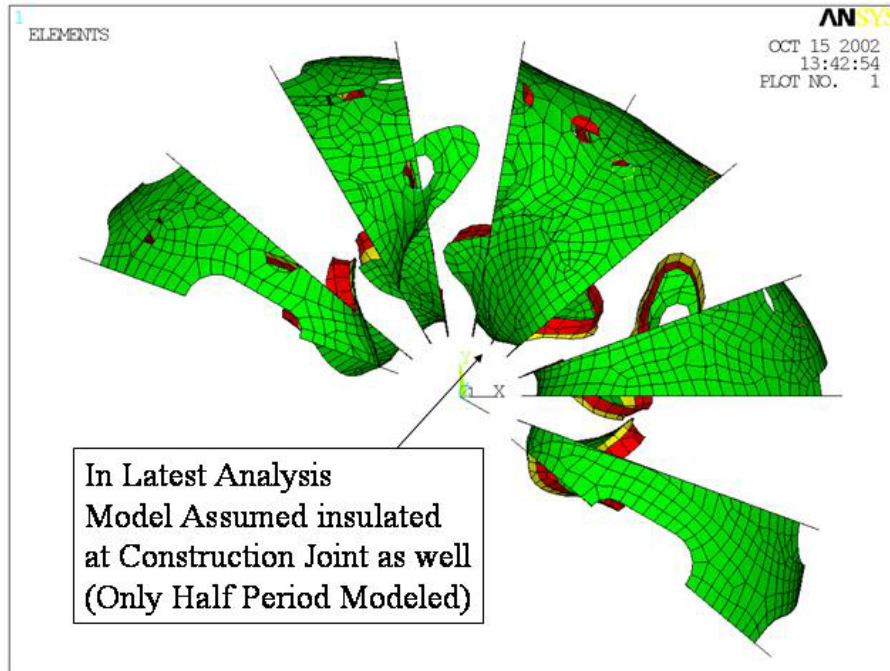
ProE Surface Model of Modular Coil Support – Shell and Tee



Spark Model with Poloidal Break (viewed by ANSYS)



Exploded View of 1 Period Assembly

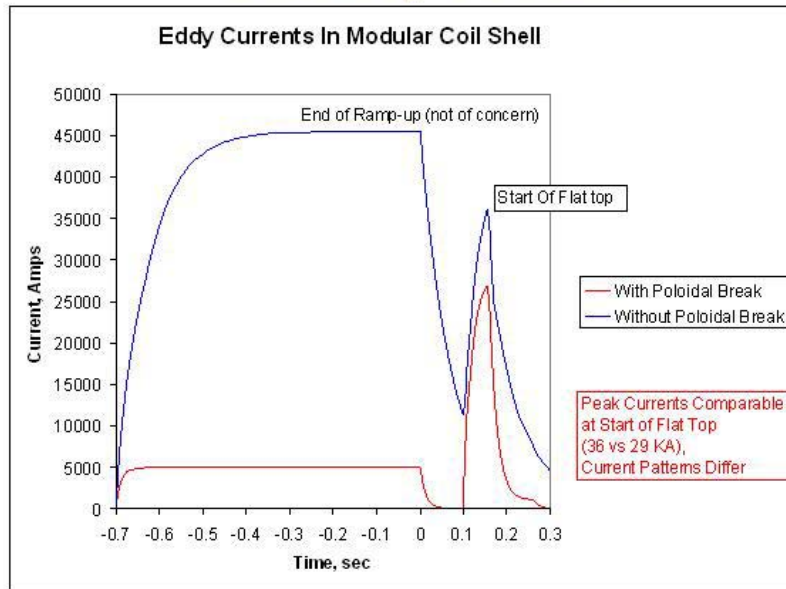


1.7T High Beta Scenario Used

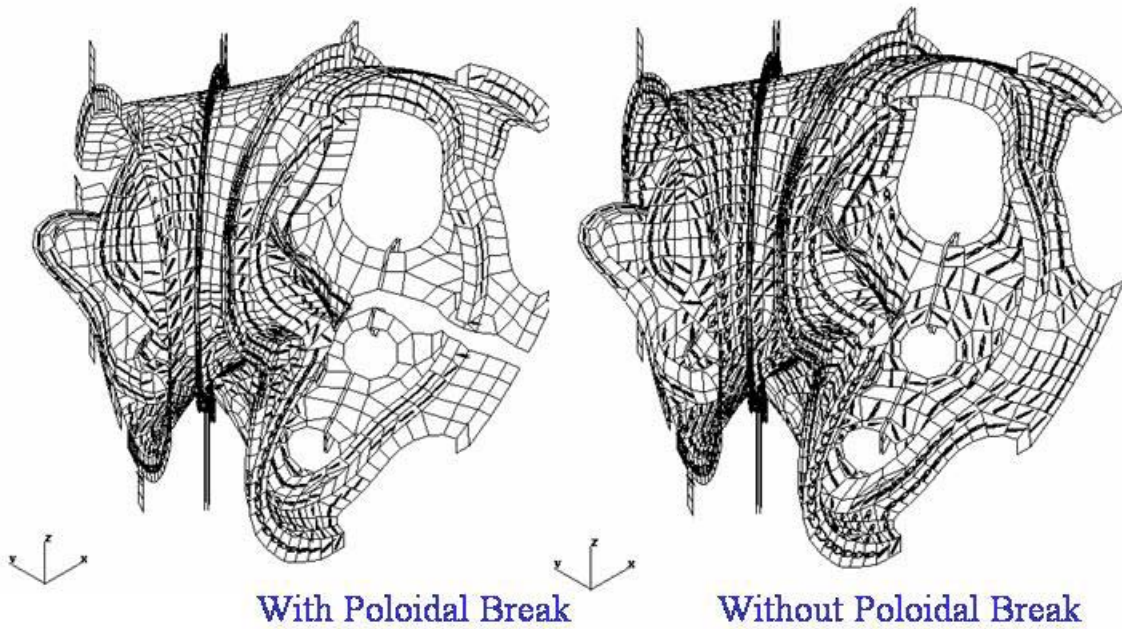
Current waveforms (A)						
	t(s)	M1	M2	M3	TF	Net
1.7T High Beta Scenario						
	-0.700	0	0	0	0	0.00
<i>High iota vacuum</i>	0.000	22139	20102	17621	-4770	11900000.00
	0.100	22139	20102	17621	-4770	11900000.00
	0.158	19292	18075	15668	2057	11900000.00
	0.258	19283	18184	15307	2320	11900000.00
	0.458	19283	18184	15307	2320	11900000.00

Current waveforms (A)		di/dt (MAT/s)				
	t(s)	M1	M2	M3	TF	Net
1.7T High Beta Scenario						
	-0.700	0	0	0	0	0.00
<i>High iota vacuum</i>	0.000	6.832	6.203	5.437	-1.472	17.000
	0.100	0.000	0.000	0.000	0.000	0.000
	0.158	-10.803	-7.548	-7.275	25.425	0.000
	0.258	-0.021	0.234	-0.780	0.567	0.000
	0.458	0.000	0.000	0.000	0.000	0.000

Max Eddy Currents



Spark Current Distribution at t=0.158s



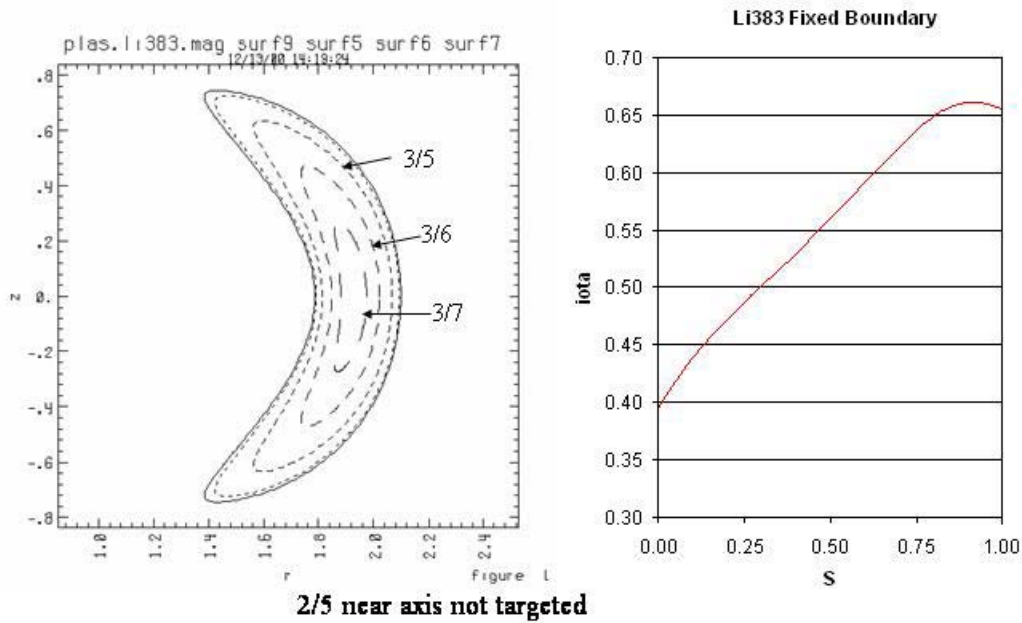
Error Fields and Resultant Islands

Mode		Island Size, ds (Percent Total Flux)	
		With Poloidal Break	Without Poloidal Break
m	n		
5	3	4.06%	9.35%
10	6	1.01%	2.30%
6	3	4.13%	6.29%
12	6	0.45%	0.60%
7	3	0.32%	0.80%
14	6	0.04%	0.07%
Estimated Total		8.50%	16.44%
Bmax, Gauss		241	878
Time Constant, ms		15.9	69.3

Note: Large Error Field (Bmax) may invalidate linear perturbation assumption inherit in Island Size Calculation

Estimated Total based on sum of dominate mode on each surface

Li383 Targeted Resonances



Island Width Evaluation used in VACISLD using VMEC data

Using s, θ, ϕ as the magnetic coordinates, island width given by:

$$ds = 4 \left| \frac{C_{ms}(s)}{m \iota'(s)} \right|^{1/2}$$

where $C(s) = \frac{B^s}{B^\phi} = \frac{B \cdot \nabla s}{B \cdot \nabla \phi}$

$\frac{B^s}{B^\phi}$ is evaluated by making use of

$$B^\phi = \frac{1}{J_{s,\theta,\phi}} \frac{dY}{ds}$$

and $\nabla s = \frac{1}{J_{s,\theta,\phi}} \left(\frac{\partial \mathcal{R}}{\partial \theta} \times \frac{\partial \mathcal{R}}{\partial \phi} \right)$

leaving an expression which does not require explicit evaluation of the Jacobian and linear in B (and therefore coil currents)

$$\frac{B^s}{B^\phi} = \frac{B \cdot \left(\frac{\partial \mathcal{R}}{\partial \theta} \times \frac{\partial \mathcal{R}}{\partial \phi} \right)}{\frac{dY}{ds}}$$

Summary

- Field Errors at Start of Flat Top Significant and more than 3.5 times Larger without Poloidal Break
- Islands Induced result in twice as much flux loss
- Significantly longer time constant without Poloidal Break implies more of flat top will be lost
- Due to large field errors, equilibrium should be recalculated to properly assess impact

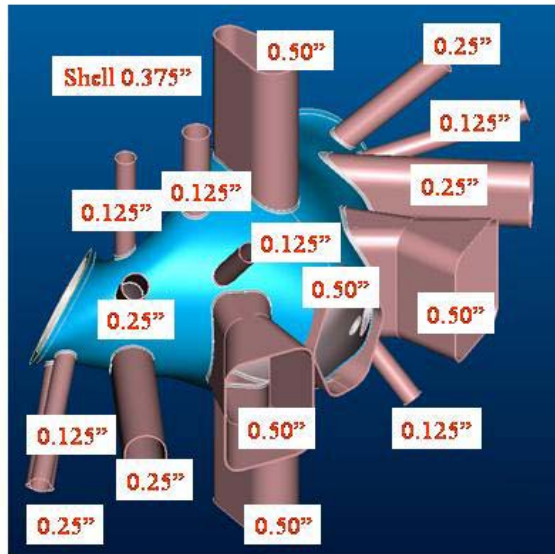
3.2.2 Vacuum Vessel

The Vacuum Vessel is required to have a time constant of less than or equal to 10 ms. A SPARK eigenvalue analysis was carried out for the 3/8 Inconel VV shell with all its ports. The slowest (i.e. longest) time constant was found to be 5.3 ms. Having met the stated requirement, no error field analysis was done.

The SPARK analysis was based on the Pro/E geometry depicted below. A model developed by Fred Dahlgren for structural analysis was converted to SPARK format and exercised. The model size, ~8000 elements, is presently near the limit of what can be run within the 2-GB memory currently available on our workstations. The SPARK eigenvalue solver was based on an old NAG subroutine, which would have required even more memory before conversion to a more modern and efficient algorithm which fit within our available memory.

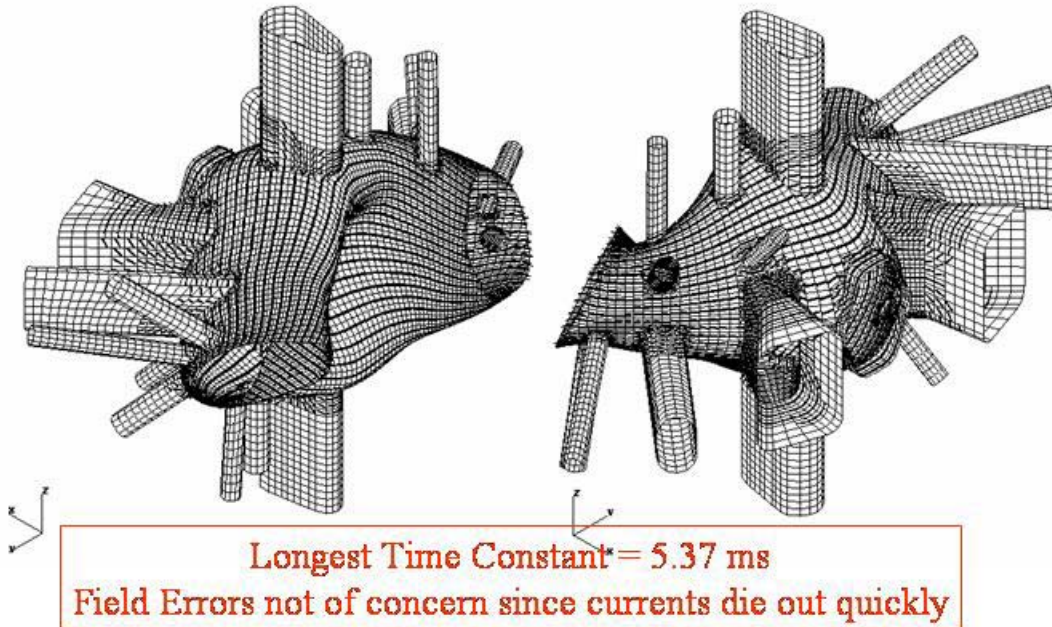
The dominant mode is predominately toroidal current flow with some net poloidal current flow producing a helical current pattern as it circulates around the vacuum vessel.

Thicknesses of Shell and Ports



Material:
Inconel
Resistivity:
130.e8 ohm-m

SPARK Eigenvalue Solution



3.2.3 Existing Copper Floor (Ground Plane)

The proposed site for the NCSX test cell is the former home to the PBX and PLT experiments. The building was constructed with a copper grounding sheet covering the entire floor. This copper floor poses some concern for operation of NCSX since eddy currents will be induced as in any other structure and the time constant is expected to be fairly long relative to other components. Removing the copper sheet and installing a new grounding plane less susceptible to eddy currents would be an expensive proposition. The alternative of cutting breaks into the copper sheet to break up eddy current paths and reduce the field errors, was explored. Based on prior experience with copper sheet, it was not expected that the floor could be segmented fine enough to reduce time constants below 20 ms where field errors could be ignored.

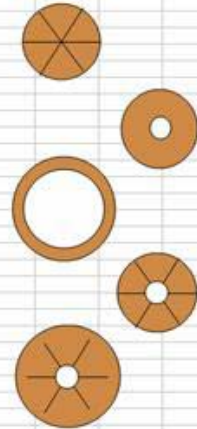
Several schemes involving simple straight line cuts were investigated. To preserve stellarator symmetry in the geometry and thus the field errors from induced eddy currents, radial cuts thru the center of the machine location were considered. The number and length of these cuts were varied. In addition, partial removal of the copper floor under the machine was considered. The copper floor extends under shield blocks along the perimeter of the room, most of which are to be re-used so we would prefer not to have to move them. Not doing so would leave loops around the machine, albeit far from the center of the machine. This effect was also investigated.

The table with figures below summarizes the finding. For each configuration, SPARK was run using as a driver the 1.7 T High Beta configuration as previously described in Section 3.2.1. The eddy currents and resultant field errors at the start of flattop were again most significant.

Results of this analysis led to the conclusion that the floor must be cut into 12 radial or 6 diametric cuts (i.e. every 30 deg). Remote loops were shown to be a concern, so the cuts must extend to the end of the floor at least in three locations (to preserve stellarator symmetry). It is expected that the length of the 9 remaining radial cuts can be reduced but should extend at least under the footprint of the machine (~3 m). Verification of this is work to be done (TBD).

Field Errors from Copper Floor Segmentation Scheme Options

PF coils only (expected to be most significant)										
1.9 Tesla High Beta Equilibrium with Max Dipole Rate of Change of 5.0e7 a-m2/s from Wayne's Technical Data Sheet TDS_C07R00_E										
1/6" Copper Floor	Configuration			Eddy Currents	Field Errors					Model id
	Number of Radial Cuts	Outer Radius, m	Inner Radius, m	Max Current, amps	Max Field Error, G at Plasma	3/5 Island Size, % Flux	3/6 Island Size, % Flux	3/7 Island Size, % Flux	1/2 Island Size, % Flux	
No Cuts	0	10	0.1	37502	18.2	3.90	1.20	0.20	0.00	12e
Radial Cuts	6	10	0.1	7667	3.1	1.50	0.49	0.08	0.00	6
	8	10	0.1	5780	2.24	1.29	0.42	0.06	0.00	8
	12	10	0.1	3650	1.23	0.95	0.30	0.05	0.00	12
No Cuts	0	20	0.1	39050	18.7	3.92	1.18	0.20	0.00	12d0e
Central Hole Under Machine	0	20	1	37457	18.6	3.92	1.18	0.20	0.00	12r1e
	0	20	2	33327	18.1	3.82	1.16	0.20	0.00	12z2e
	0	20	3	28082	16.4	3.54	1.10	0.18	0.00	12z3e
Impact of Remote Loops	0	20	10	7476	3.38	1.09	0.05	0.06	0.00	12r10e
	0	11	10	4137	2.14	0.89	0.40	0.05	0.00	12r11e
	0	12	11	3488	1.69	0.76	0.36	0.04	0.00	12r12e
	0	10.5	10	3142	1.54	0.79	0.35	0.04	0.00	12r13e
Radial Cuts Only	12	20	0.1	3588	1.47	1.08	0.34	0.05	0.00	12d
Cuts and Central Hole	12	20	1	3569	1.47	1.07	0.34	0.05	0.00	12r1
	12	20	2	2927	1.00	0.79	0.29	0.04	0.00	12z2
	12	20	3	1571	0.50	0.53	0.21	0.03	0.00	12z3
Partial Radial Cuts	12	20/10	2	11238	6.82	1.90	0.72	0.10	0.00	12z2p
Full Cut (repeat of case 12z2)	12	20/20	2	2927	1.00	0.79	0.29	0.04	0.00	12z2
No Cut (repeat of case 12z2e)	12	20/0	2	33327	18.1	3.82	1.16	0.20	0.00	12z2e



3.2.4 Machine Base Plates

Relocating and re-using the existing steel base plates from the PBX machine support had been proposed. These are 2 roughly 2m x 4m x 0.1m (4 inches) thick ferromagnetic steel plates sitting side by side on the machine floor. While they pose a potential problem due to the large amount of ferromagnetic material close to the machine, they also pose another concern with field errors from induced eddy currents. Since this problem is easier to handle it was addressed first.

Using methods and conditions described for the copper floor in the previous section and Section 2, the field errors were evaluated. Results showed large field errors at the plasma (4 Gauss average and 10.5 Gauss max B.n) and islands totaling 4.3%. As a result, it was decided not to re-use these plates.

3.3 FERROMAGNETIC MATERIAL

3.3.1 Neutral Beam Magnets

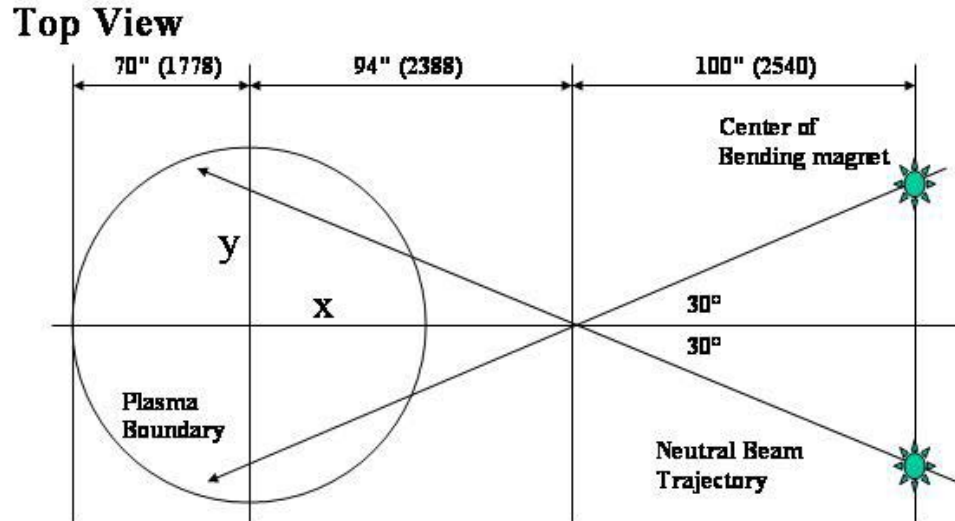
The Neutral Beams being re-used from PBX contain at large bending magnetic wound around a ferromagnetic core to concentrate the field used to control non-neutrals on the beam. This posed a concern from two standpoints:

- 1) Does the stray field from the bending magnetic produce significant field errors at the plasma?
- 2) Does the remote field from the Stellarator Core magnetics further magnetize the ferromagnetic material at the NB significantly contributing to field errors at the plasma?

To answer these questions, an ANSYS model of the Neutral Beam Bending Magnet was constructed and run by Chang Jun. The self-field from the bending magnetics and ferromagnetic core during Neutral Beam Operation was evaluated at discrete points on the resonant surfaces in the plasma. Using the VACISLD Code, the resonant component of the normal field on the surface was evaluated and the island size calculated. Similarly, the field from the ferromagnetic core subjected to a background field from the stellarator core magnetics was evaluated at the plasma. This was done with and without the NB operating.

The resultant field errors were found to be less than 1 gauss. Predicted flux lost to islands was dominated by the $m=2$ mode with islands of 1.0%.

Positioning of NCSX NB Assy



Magnetic Field Analysis

- Neutral beams pass through the bending magnets (BM) to be filtered off positive ion.
- CONCERN-1: Stray magnetic field from BM could affect on plasma surface & change the shape. (BM field only)
- CONCERN-2: The field from plasma & coils can change the magnetization of BM iron. This plasma field can also affect on the plasma itself – “boomerang” effect. (BM field + plasma field)
- CONCERN-3: When BM is turned off, the plasma’s boomerang effects could be more harmful than driving time. So this case is also calculated. (plasma field only)

the Conditions of Analysis

- There are total 4 sets of BM:
Two at $0 \pm 17^\circ$ (1. $x=4.9\text{m}$, $y=1.5\text{m}$)
(2. $x=4.9\text{m}$, $y=-1.5\text{m}$)
Two at $-120 \pm 17^\circ$ (3. $x=-1.10\text{m}$, $y=-4.77\text{m}$)
(4. $x=-3.58\text{m}$, $y=-3.34\text{m}$)
- Only two sets (above 1. & 2.) are included in ANSYS analysis & effects from other two sets are calculated by the consideration of cyclic symmetry after ANSYS run.
- Two sets are considered in ANSYS, but the FE model bears only a half of BM (upper part of 1.). $X=0$ surface is flux perpendicular boundary, $z=0$ surface is flux parallel boundary & other surrounding surfaces are flux parallel one.

ANSYS Model & Results (CASE-1)

- CASE-1: Only BM effect on plasma is calculated.
- ANSYS results: Please confer attached figures.
- After ANSYS: the surface points of plasma are not matched with nodes points of ANSYS model. So, interpolation calculations are coded with C++ and done as follows:
 - 1) Renumbering of nodes and elements: make nodes & elements start from zero and delete any space between numbers.
 - 2) Arranging node order: sort by positions in elements.
 - 3) Finding affiliation: to judge that each plasma point includes which element.
 - 4) Interpolation by surrounding 8 node points: By shape functions.
 - 5) Cyclic symmetry calculation for the other 2 BM effect on plasma.

ANSYS Model & Results (CASE-2)

- CASE-2: BM + plasma field is calculated on plasma.
 - 1) Art Brooks calculated the m-field on BM by the plasma & coils.
 - 2) I found that the field characteristic is very similar with a field generated by a straight coil on $x=4.53\text{m}$ bearing $35,000.0\text{A}$ from $+z$ to $-z$ (Art's results at the center of 1st and 2nd BM are as follows:
 $x=4.9\text{m}$, $y=1.5\text{m}$, $z=0.0\text{m}$: $B_x=4.30\text{E-}3$, $B_y=-1.05\text{E-}3$, $B_z=-5.17\text{E-}4$ T
 $x=4.9\text{m}$, $y=-1.5\text{m}$, $z=0.0\text{m}$: $B_x=-4.30\text{E-}3$, $B_y=-1.05\text{E-}3$, $B_z=-5.17\text{E-}4$ T)
- ANSYS analysis: Please confer attached figures.
 - 1) A straight coil is inserted in ANSYS model with BM iron
 - 2) The same model was done with iron.
- In interpolation procedure, final results have 1) – 2) values.

ANSYS Model & Results (CASE-3)

- CASE-3: plasma & coils field on BM and returning effect on plasma.
- Every calculation steps are same as case-2.
- But, BM race track coils bear zero current.
- This case is to evaluate the magnetic field on plasma when the BM was turned off.
- Because of non-linear behavior, the results of CASE-2 does not match with the results of CASE-1 + CASE-3.
- ANSYS results: Please confer attached figures.

Results Analysis & Conclusion

- By 2 sets of BM, B_y is dominant at the nearest part of plasma (at $x > 1\text{m}$). Maximum stray field is less than 1gauss or $1.0\text{E-}4$ Tesla.
- When 4 sets are considered, B_x goes up and B_y is down at the nearest plasma zone, but still the field magnitude is less than 1gauss.
- The returned magnetic field by plasma & coils through BM iron is more important than the stray field that the BM generates.
But, the field is still less than 1gauss.
- The returned field when BM is turned off is most important comparing other cases because BM field by its own current & m-field by plasma has opposite signs. But, the field is still less than 1gauss.
- The plasma & coils disturb the m-field inside the BM only by less than 1%. Therefore, BM function will not be affected by the plasma.

3.3.2 Building Steel (TBD)

3.3.3 Other (TBD)

3.4 DIAGNOSTICS (TBD)